Since January 2020 Elsevier has created a COVID-19 resource centre with free information in English and Mandarin on the novel coronavirus COVID-19. The COVID-19 resource centre is hosted on Elsevier Connect, the company's public news and information website.

CHAPTER SIX

Cubic Membranes: The Missing Dimension of Cell Membrane Organization

Zakaria A. Almsherqi,[*] Tomas Landh,[†] Sepp D. Kohlwein,[‡] *and* Yuru Deng[*]

Contents

* Department of Physiology, Yong Loo Lin School of Medicine, National University of Singapore, 117597 Singapore
† Novo Nordisk A/S, DK-2760 Måløv, Denmark
‡ Institute of Molecular Biosciences, University of Graz, A8010 Graz, Austria

International Review of Cell and Molecular Biology, Volume 274
ISSN 1937-6448, DOI: 10.1016/S1937-6448(08)02006-6

Abstract

Biological membranes are among the most fascinating assemblies of biomolecules: a bilayer less than 10 nm thick, composed of rather small lipid molecules that are held together simply by noncovalent forces, defines the cell and discriminates between "inside" and "outside", survival, and death. Intracellular compartmentalization—governed by biomembranes as well—is a characteristic feature of eukaryotic cells, which allows them to fulfill multiple and highly specialized anabolic and catabolic functions in strictly controlled environments. Although cellular membranes are generally visualized as flat sheets or closely folded isolated objects, multiple observations also demonstrate that membranes may fold into "unusual", highly organized structures with 2D or 3D periodicity. The obvious correlation of highly convoluted membrane organizations with pathological cellular states, for example, as a consequence of viral infection, deserves close consideration. However, knowledge about formation and function of these highly organized 3D periodic membrane structures is scarce, primarily due to the lack of appropriate techniques for their analysis *in vivo*. Currently, the only direct way to characterize cellular membrane architecture is by transmission electron microscopy (TEM). However, deciphering the spatial architecture solely based on two-dimensionally projected TEM images is a challenging task and prone to artifacts. In this review, we will provide an update on the current progress in identifying and analyzing 3D membrane architectures in biological systems, with a special focus on membranes with cubic symmetry, and their potential role in physiological and pathophysiological conditions. Proteomics and lipidomics approaches in defined experimental cell systems may prove instrumental to understand formation and function of 3D membrane morphologies.

1. Introduction

Membrane-bound cell organelles are typically considered to have rather spherical topology, delineated by one phospholipid-bilayer membrane that separates the interior from the exterior. However, this simplification of organelle topology is a rule not a law, and it is well known that a large number of membrane structures exists in Nature with more complex 3D morphologies. Indeed, the topology of membrane-bound organelles is a rather unexplored area of research. This might be due to

difficulties in obtaining information about topological parameters from living or fixed cells, and the interpretation of these parameters in the cellular context. Nevertheless, the importance of topology considerations, for example, subcellular compartmentalization, transport phenomena, and sorting events that involve membrane trafficking processes is evident. Cell membrane morphology, controlled by the principles of self-assembly and/or self-organization, is likely to adopt an optimally organized structure under the influence of selective conditions. This is a dynamic process, perhaps restricted to sub-membrane domains, and short-lived, and is dependent on the lipid as well as protein components of the membrane.

As a consequence of limited *in vivo* technologies, knowledge about the molecular mechanisms underlying membrane morphology is scarce and largely restricted to the descriptive level. Indeed, higher order membrane topologies identified by transmission electron microscopy (TEM), are frequently reported in the literature, yet due to their very heterogeneous representations, common features are difficult to comprehend. Among these nonlamellar cell membranes, especially cubic membrane organizations attract great attention (Almsherqi *et al.*, 2006; Hyde *et al.*, 1996; Landh, 1995, 1996) because of their unique feature of 3D periodicity in TEM micrographs and great similarity to the bicontinuous lipidic cubic phases (Bouligand, 1990; Larsson, 1989; Larsson *et al.*, 1980; Luzzati, 1997). Cubic membranes (Figs. 6.1 and 6.2) have therefore often been compared to self-assembled cubic lipidic phases in aqueous dispersions that are well

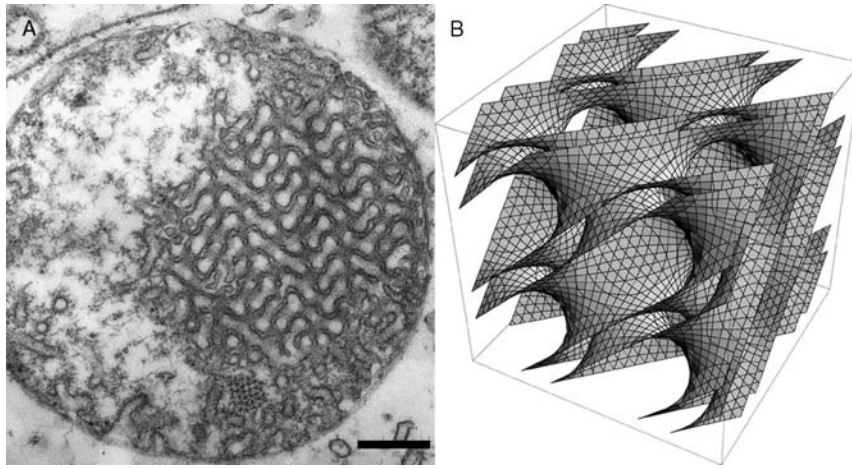

Figure 6.1 Cubic membrane architecture (Almsherqi *et al.*, 2008). (A) Two-dimensional transmission electron micrograph of a mitochondrion of 10 days starved amoeba *Chaos* cells and (B) three-dimensional mathematical model of the same type of cubic membrane organization. Scale bar: 250 nm.

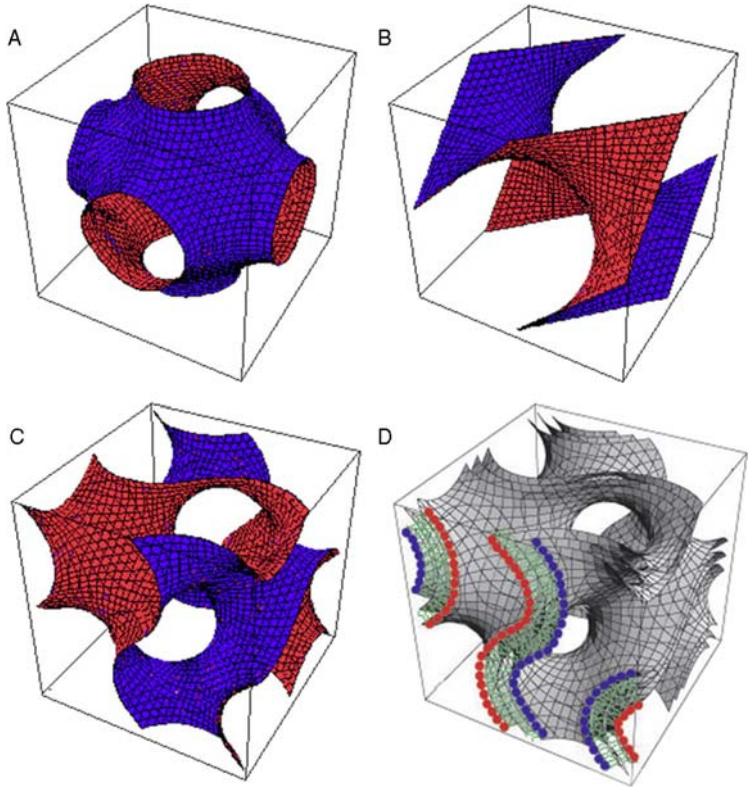

Figure 6.2 Periodic cubic surfaces and cubic membrane. Oblique views of the unit cell of (A) Primitive, (B) Double Diamond, and (C) Gyroid cubic surfaces observed in biological systems. (D) The bilayer constellation of a 3D mathematical model of a cubic membrane. Three parallel Gyroid-based surfaces can be used to describe a biological membrane (bilayer), in which case the centered surface is the "imaginary" hydrophobic mid-bilayer surface and the two parallel surfaces are the two apolar/polar (interfacial) surfaces.

characterized *in vitro*, with several applications. Indeed, the efforts toward understanding formation and functional roles of cubic membranes in biological systems have been paralleled by the efforts in investigating cubic phases formation and their behavior in lipid–water systems.

2. Cell Membrane Architecture

2.1. Membrane symmetries

Biological membranes may exhibit point or line symmetry. A membrane is symmetrical if it can be nontrivially rotated, inverted, mirrored, and translated such that it is indistinguishable from its initial appearance. Symmetry of

biological membranes is mainly described by rotations. Several sets of membrane arrangements exhibit symmetry such as parallel membranes and hexagonal packing of tubes. In contrast, a cubic membrane exhibits distinct morphological patterns when projected which may even be translated into unique signatures in many directions (Fig. 6.3). The patterned membrane organization of cubic membranes consists of a network arranged in a nonrandom order and is evenly spaced. Therefore, through an overall inspection of TEM micrographs, cubic membranes are recognized via perceptual cues of the patterned membrane organization (Almsherqi *et al.*, 2006; Landh, 1996). This unique appearance of cubic membranes in TEM micrographs frequently allows for the differentiation of cubic membrane organization from other membrane arrangements such as tubulo-reticular structures (TRS) and annulate lamellae (AL) (Figs. 6.4 and 6.5).

Cubic membranes represent highly curved, 3D periodic structures that correspond to mathematically well-defined triply periodic minimal surfaces or the corresponding periodic nodal surfaces and their respective constant mean curvature or level surfaces (Fig. 6.2). Both the latter surface descriptions are approximative descriptions of surfaces parallel to the minimal or nonzero level surface (Landh, 1996). Cubic membranes have been detected

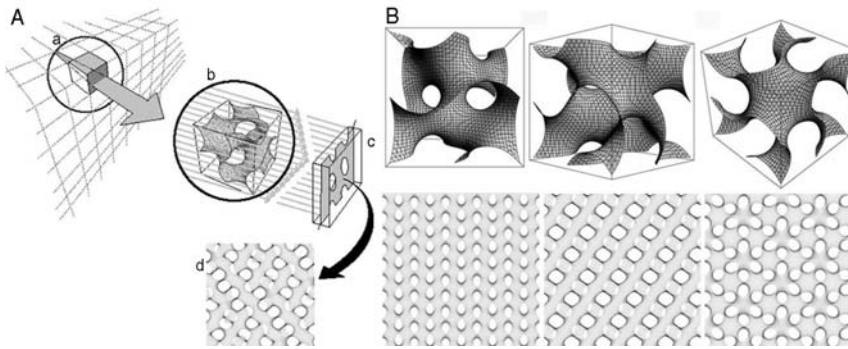

Figure 6.3 Computer simulation of TEM images. (A) Schematic illustration of TEM data in 2D projections of a specimen with a finite thickness. A 3D object (a) is depicted and is translucent to the projection rays of an electron beam; (b) representation of one unit cell of the gyroid surface; (c) projection plane onto which the rays impinge, in analogy of the film on which the image would be recorded; (d) 2D projection map provides a corresponding template for matching the patterned membrane domain in the TEM micrograph. (B) Comparison between a 3D cubic membrane model of a gyroid-based surface and its computer simulated projections at different viewing directions. Multiple 2D projections that are generated from the same 3D structure form a library of different patterns. The bottom row corresponds to computer-simulated projections for the top row, based on a projected specimen thickness of one-half of a unit cell viewed at the [1, 0, 0] (left), [1, 1, 0] (middle), and [1, 1, 1] (right) directions. The computer-generated projection can be matched with TEM micrographs to determine the 3D structure of a cubic membrane arrangement (see section 2.4. for further details).

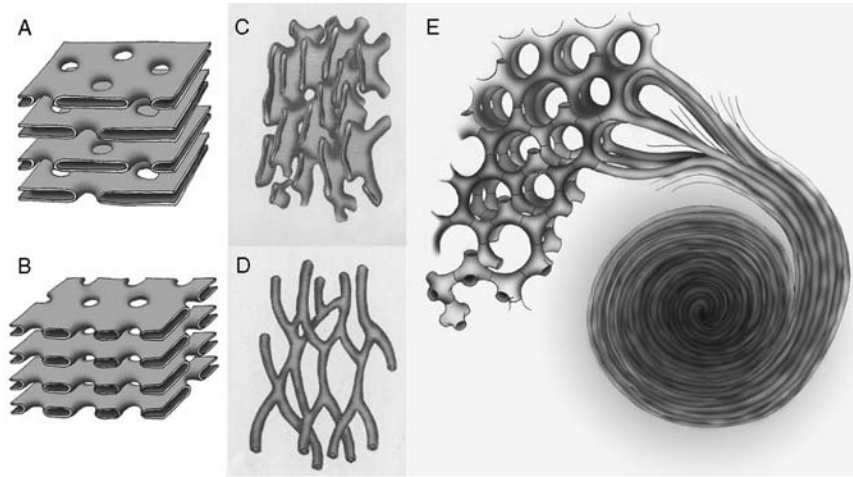

Figure 6.4 Cell membrane organization. Schematic diagram depicting the likely 3D structure of annulated lamellae, tubulo-reticular structure (TRS) and the membrane folding transition. The pores of annulated lamellae may alternate in arrangement with the symmetry often being quadratic (A) or the pore face each other with the symmetry being hexagonal (B). Two examples of TRS membrane arrangements; (C) interconnected sacular (cisternae) and (D) tubular membrane organization show no global symmetry. A possible model of continuous membrane folding for the formation of double diamond (lower left) and gyroid (upper left) cubic type, hexagonal (upper right) and lamellar structures, and whorls (lower right) (E). The coexistence of these membrane organizations has been reported frequently in UT-1 and COS-7/CV-1 cells with HMG-CoA reductase and cytochrome b(5) overexpression, respectively. Panels A-D adapted from Figs. 17 and 18; Bouligand, 1991.

without any obvious restrictions or preferences in all kingdoms of life, both under physiological or pathological conditions (Table 6.1). They appear not to be limited to certain types of cells, although they may occur more frequently in some cell types. Furthermore, cubic membranes are not strictly associated with any particular organelle and can apparently evolve from almost any cytomembrane: plasma membrane, endoplasmic reticulum (ER), nuclear envelope (NE, both inner (INE) and outer (ONE)), inner mitochondrial membrane, and the Golgi complex. The smooth ER, however, seems to be the organelle most frequently associated with cubic membrane formation. So far, three surface families have been identified to exist, and these three types of cubic membranes are schematically shown in Fig. 6.2. They are designated according to their corresponding triply periodic minimal (or level) surfaces as gyroid (G), double diamond (D), and primitive (P) surfaces.

Cubic membranes often coexist with other "unusual" membrane arrangements, such as TRS, which are irregularly arranged tubes that bifurcate and reanastomose. In many cases, these tubes show a preferential

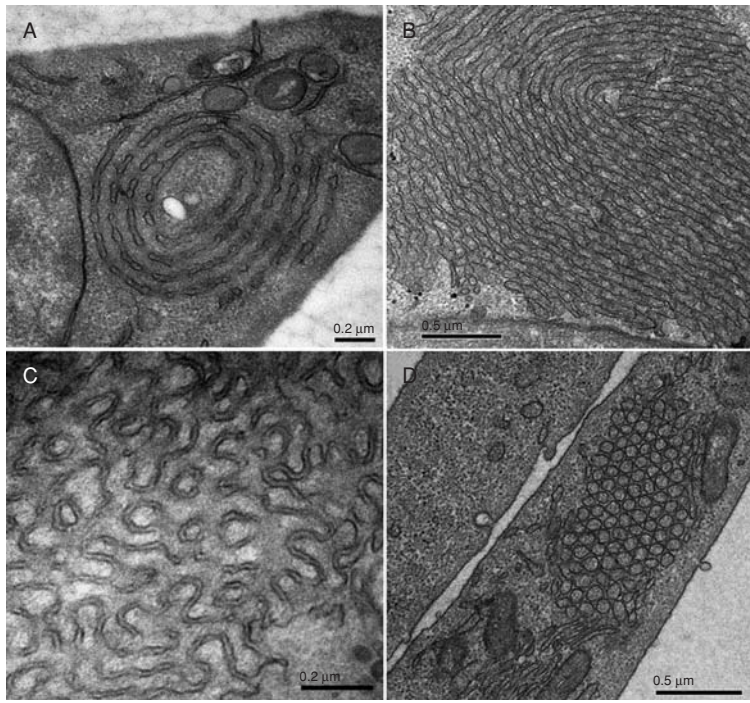

Figure 6.5 Examples of different membrane organizations observed in UT-1 cells, 48–72 h after compactin (40 μM) treatment (Deng *et al.*, unpublished). (A) Annulate lamellae, (B) stacked undulated lamellae that show hexagonal transition, (C) cubic, and (D) hexagonal membrane morphologies may coexist in the same cell. Membrane folding appears to originate at the nuclear envelope or the endoplasmic reticulum.

orientation. The main difference of TRS to cubic membranes is that TRS symmetry is usually nematic, since the layers do not show obvious periodic distribution (Fig. 6.4D). The preferential alignment along a direction may be due to an elongation process, perhaps in association with the cytoskeleton, and is not necessarily the result of a spontaneous membrane alignment. However, there are many cases in which the periphery of a perfectly preserved cubic morphology shows TRS appearance, which, therefore, may be introduced by the fixation method (Landh, 1995). Membranes of true cubic morphology are often mis-labeled as TRS in the literature, due to the convoluted image projections observed for both structures. Many of the examples listed in Table 6.1 have been designated as TRS, despite the presence of a distinct cubic symmetry (Almsherqi *et al.*, 2005; Landh, 1996). TRS have attracted biomedical interest due to their potential use as an ultrastructural marker for pathological conditions: they occur in virus-infected and in cancer cells and have been, therefore, often regarded as an

Table 6.1 Occurrence of cubic membranes in biological systems.

Description of cells/tissue	Cognomes	S''/a (nm)	References
Monera			
Gracilicutes			
Oxyphotobacteria			
Cyanobacteria			
Thylakoid lamellae in *Anabaena* sp.		D/50	Lang and Rae (1967)
Thylakoid lamellae in *Anabaena* sp.			Beams and Kessel (1977)
Thylakoid lamellae in Heterocyst of *Anabaena azollae*	Honeycombed lamellae		Lang (1965)
Thylakoid in *Anabaena variablis* infected with cyanophages	PLB-like structure	P/300	Granhall and von Hofsten (1969)
Protista			
Algae			
Clorophyta			
Chlorophyceae			
Membranes in chloroplasts of *Zygnema*	Quasi-crystalline lamellar	P^m/350	McLean and Pessoney (1970)
Membranes in chloroplasts of *Zygnema*		G^m/500	Deng and Landh (1995)
Thylakoid membranes in chloroplast of C-10 mutant of *Chorella vulgaris*	Masses of prethylakoid tubules		Bryan *et al.* (1967)
Thylakoid membranes in chloroplast of *Protosiphon botyoides*	Sinusoidal thylakoids		Berkaloff (1967)
Charophyceae			
Plasma membrane of *Chara coralline, C. braunii*	Charasome	G/140	Barton (1965), Franceshi and Lucas (1980, 1981), Lucas and Franceshi (1981)

Plasma membranes of *Nitella*	Interconnected tubules	G	Crawley (1965)
Rhodophyta			
Rhodophyceae			
ER in *Erythrocystis montagnei*	Crystalline body		Tripodi and de Masi (1977)
Gymnomycota (Myxomycota, slime moulds)			
Plasmodiogymnomycotina			
Myxomycetes			
Mitochondria in *Physarum polycephalum*	Regular tubular network	D^2	Daniel and Järlfors (1972a,b)
Mitochondria in *Didymium nigripies*	Unusual tubular morphology	D^2	Schuster (1965)
Mastigomycotina			
Diplomastigomycotina			
Oomycxetes			
ER in *Oedogoniomyces zoospores*	Organized lamellar system	G/215	Reichle (1972)
Protozoa			
Sarcomastigophora			
Mastigophora			
Phytomastigophora			
Photosynthetic lamellae in dark-grown *Chlamydomonas reinhardi* y-1	Meshed network, PLB-like		Friedberg *et al.* (1971) Hoober *et al.* (1969)
Zoomastigophorea			
ER in *Leptomonas collosoma*	Membrane lattice	D/88	Linder and Staehelin (1980)
Rhizopodea			
Amoebida			
Mitochondria in *C. carolinense*		D^2/150	Pappas and Brandt (1959), Brandt and Pappas (1959), Borysko and Roslansky (1959), Daniels and Breyer (1968)

(*continued*)

Table 6.1 (*continued*)

Description of cells/tissue	Cognomes	S^n/a (nm)	References
Mitochondria in *C. carolinense*[a]		D^2, P^2/130	Deng and Mieczkowski (1998); Deng *et al.* (1999)
Mitochondria in *Chaos illinoisensis*	Complex tubular patterns	D^2	Daniels and Breyer (1965)
Pelobiontida			
Intranuclear membrane in *Pelomyxa palustris*	Crystalloid		Daniels and Breyer (1967)
Cnidospora			
Microsporidea			
Membranes in sporoblast of *Nosema apis*	Honeycomb network		Youssef and Hammond (1971)
Ciliophora			
Oligohymenophora			
Hymenostomatida			
Pniculina			
Contractile vacuolar membranes of *Paramecium aurelia, Paramecium multimicronucleatum*	Smooth spongiome		Mckanna (1976), Allen and Fok (1988), Allen *et al.* (1990), Fok *et al.* (1995), Hausmann and Allen (1977), Ishida *et al.* (1993, 1996)
Intranuclear membrane of *Neobursaridium gigas*	Crystal configuration	G/160	Nilsson (1969)
Tetrahymenina			
Contractile vaculor membranes of *Tetrahymena pyriformis*	Nephiridial tubules		Elliott and Bak (1964)
Fungi			
Amastigomycota			
Ascomycotima			

Ascomycetes			
ER in apothelial cells of *Ascobolus stercorarius*	Lattice bodies	G/55	Anderson and Zachariah (1972), Zachariah (1970), Zachariah and Anderson (1973), Wells (1972)
Plant			
Pteridophyta			
Oocytes in *Selaginella kraussiana*	Pseudocrystal		Robert (1969a,b)
Sprematohyta			
Angiosperms			
Magnoliophyta (anthophyta)			
Dicotyledons			
Ranunculidae			
Ranunculaceae			
ER of nectaries in *Helleborus foetidus*	Cotte de mailles	$P^2/80$	Eymé (1963, 1966), Eymé and Blance Le (1963)
ER of ovules in *Ficaria ranunculoides*	Cotte de mailles	P	Eymé (1966, 1967)
ER in virus-infected leaf parenchyma cell of *Helleborus niger*	ER complex	$P^2/65$	Robinson (1985)
ER in phloem-parenchyma cells of *Helleborus lividus*	ER complex	$P^2/75$	Behnke (1981)
ER in differentiating sieve elements of *Eranthis cilicica*	ER complex	$G^2/70$, 145	Behnke (1981)
Papaveraceae			
ER in ovules of *Papaver rhoeas*	Cytoplasmic complex	P^2, D^2	Ponzi *et al.* (1978)
Hamamelididae			
Urticales			
ER in differentiating sieve elements of *Ulmus americana*	Complex network/maize		Evert and Deshpande (1969)

(*continued*)

Table 6.1 (*continued*)

Description of cells/tissue	Cognomes	S^n/a (nm)	References
Caryophyllidae			
Caryophyllales			
ER in sieve elements of beet yellow vein virus infected *Beta*	Convulated ER		Esau and Hoefert (1980)
Dilleniidae			
Capparales			
ER in nectaries of *Diplotaxia erocoides*	Cotte de mailles	$P^2/55$	Eymé (1966, 1967)
Malvales			
ER in differentiating sieve elements of *Gossypium hirsutum*	Convoluted ER		Thorsch and Esau (1981)
Rosidae			
Leguminosae			
Plastids in bean root tips of *Phaseolus vulgaris*	Tubular complex		Newcomb (1967)
ER in differentiating sieve element of *P. vulgaris*	Convoluted membranes		Esau and Gill (1971)
Sapindales			
ER in differentiation sieve elements of *Acer*	Quasi-crystalline membranes	$D^2/180$	Wooding (1967)
ER in differentiation sieve elements of *Acer pseudoplatanus*	Vesicular aggregates		Northcote and Wooding (1966)
Asdteridae			
Gentianales			
ER in differentiating sieve element of *Nymphoides peltata*	Convoluted membrane complex	$G^2/125$	Johnson (1969), Oparka and Johnson (1978)
Monocotyledons			
Commelinidae			
Poales			

Poacea (Gramineae)			
ER in *Triticum aestivum* infected by wheat spindle streak mosaic virus	Membranous body	G^2	Hooper and Wiese (1972), Langenberg and Schroeder (1973)
Liliidae			
Liliales			
ER of differentiating sieve elements *Dioscorea bulbifera*	Lattice-like membrane	G/40	Behnke (1968)
ER of differentiating sieve elements *Dioscorea macroura*	Lattice-like membrane	G^1, G^2/ 30, 140	Behnke (1968)
ER of differentiating sieve elements *Dioscorea reticulata*	Lattice-like body	G/35	Behnke (1965, 1968)
ER of differentiating sieve elements *Smilax excelsa*	Convoluted ER		Behnke (1973)
Arecidae			
Arecales			
ER in differentiating sieve elements of *Cocus nucifera*	Convoluted tubular ER	G^2	Parthasarathy (1974a,b)
ER in differentiating sieve elements of *Chamaedorea pulchra*, *C. oblongata, C. elegens, Elaeis guineensis*	Convoluted tubular ER		Parthasarathy (1974a,b)
Gymnosperms			
Coniferophyta			
Conniferales			
ER in sieve cells in *Pinus strobus*	Lattice-like bodies		Murmains and Evert (1966)
ER in sieve cells in *Pinus pinea*	Vesicular aggregation		Wooding (1966)
Animalia			
Mollusca			
Cephalopoda			
Nautiloidea			

(*continued*)

Table 6.1 (*continued*)

Description of cells/tissue	Cognomes	S^n/a (nm)	References
Nautilida			
ER in retinula cells in *Nautilus macromphalus*	Tubular array of myeloid body	$P^{>10}$/550	Barber (1967), Barber and Wright (1969)
Gastropoda			
Opisthobranchia			
Nudibranchia			
ER in spermatids of *Spurilla nepolitana*	Undulating tubular body	P^2/130	Eckelbarger (1982), Eckelbarger and Eyster (1981)
Pulmonata			
Helicidae			
ER in photoreceptor cells of *Helix pomatia*	Biocrystal		Röhlich and Török (1963)
Basommatophora			
ER in spermatids of *Planorbarius corneus*	Cytoplasmic crystalloid	D^2/50	Starke and Nolte (1970)
Stylommatophora			
ER in type I photoreceptor cells of *Limax maximus*	Corrugated ER	D^2/195	Eakin and Brandenburger (1975)
Annelida			
Polychaeta			
Aphroditidae, Polynoïnae			
ER in luminous cells of *Acholoe astericola*	PER, Photosomes	D^2/250	Bassot (1964, 1966), Bassot and Nicolas (1978), Bilbaut (1980), de Ceccatty *et al.* (1977)
ER in luminous cells of *Lagisca extenuata*	PER	D^2/250	Bassot (1966)
ER of photoreceptor cells in *L. extenuata*	PER	D^2	Bassot and Nicolas (1978)

ER in luminous cells of *Harmothoe lunulata*	PER		Bassot (1985), Bassot and Nicolas (1987, 1995), Nicolas (1979, 1991)
ER of photoreceptor cells in *Arctonoe vittata*	Crystalline element		Singla (1975)
Syllidae			
ER of photoreceptor cells in *Syllis amica*	PER	$D^2/50$	Bocquet and Dhainaut-Courtois (1973)
Nereidae			
ER of inner segment in photoreceptor cells in *Nereis virens*	Paracrystalline body		Dorsett and Hyde (1968)
ER of photoreceptor cells in *Nereis limnicola*	Crystalloid body	G	Eakin and Brandenburger (1985)
Oligichaeta			
Lumbricidae			
ER in spermatids of *Eisenia foetida*	Undulating tubular body		Stang-Voss (1972)
Hirudinea			
Gnathobdeliae			
ER in photoreceptor cells of *Hirudo medicinalis*	PER		Walz (1982)
Arthropoda			
Arachnida			
Scorpions			
Mitochondria in spermatids of *Euscorpius flavicaudis*			André (1959)
Pseudoscorpions			
ER of spermatids in *Diplotemus* sp.	Highly ordered membrane		Bawa and Werner (1988)

(*continued*)

Table 6.1 (*continued*)

Description of cells/tissue	Cognomes	S^n/a (nm)	References
Crustacea			
Copepoda			
ER of retinula cell in *Macrocyclops albidus*	Elaborately wound membranes		Fahrenbach (1964)
Malacostraca			
Decapoda			
ER of spermatozoa in *Cragon septemspinosa*	Paracrystalline lattice	D^2	Arsenault *et al.* (1979, 1980)
Schwann cell processes in the ventral nerve cord of *Procambarus* sp.	Anastomosing tubular inclusion		Pappas *et al.* (1971)
Schwann cell processes in the walking limb nerves *Nephrops* sp.	Anastomosing networks		Holtzman *et al.* (1970)
Mitochondria in oocytes of *Cambarus* and *Orconectes*	Honeycombed cristae		Beams and Kessel (1963)
Isopoda			
ER in bordering cells of Bellonci organ in *Sphaeroma serratum*	Annulate lamellae	G/50	Chaigneau (1971)
Tanaidacea			
ER in sperm of *Tanais cavolinii*	Spongy/foamy cytoplasm		Cotelli and Donin (1980)
Insecta			
Apterygota			
Thysanura			
ER in rectal epithelial cells of *Petrobius maritmus*	Puzzles tridimensionnels	$G^2/120$	Fain-Maurel and Cassier (1972)
Mitochondria in intestinal cells of *P. maritmus*		$D^2/160$	Fain-Maurel and Cassier (1973)
Pterygota			
Orthoptera			
ER in spermatids of *Melanoplus diffentialis differentialis*	Textum	$P^2/250$	Tahmisian and Devine (1961)

Mitochondria in corpus allata of *Locust migratoria migratorioides*			Fain-Maurel and Cassier (1969)
Hemiptera			
ER in spermatids of *Dysdercus fasciatus*	Sinusoidal tubules	$D^2/150$	Folliot and Maillet (1965)
ER in oocytes of *Pyrrocoris apterus*	PER	$D^2/250$	Mays (1967)
ER in spermatogenic cells of *Notonecta undulata*	Anastomosing tubules		Tandler and Moribier (1974)
ER in spermatogonai a and spermatocytes of *P. apterus*	PER	$G^2/175$	Wolf and Motzko (1995)
Diptera			
Mitochondria in flight muscle cells of *Calliphora erythrocephala*	Regular fenestrated cristae		Smith (1963)
ER in photoreceptor cells of vitamin A deficient *Aedes aegypti*	Masses of membranes		Brammer and White (1969)
Lepidoptera			
SER in scale cells of butterfly *Mitoura grynea*	Membrane-cuticle unit		Chiradella (1989, 1994)
Hymenoptera			
ER in secretory cells of Dufour's gland in *Parischnogaster mellyi*	Vesicular profiles		Delfino *et al.* (1988)
Blattodea			
Mitochondrion in secretory cells of the spermatheca in *Periplaneta am.*			Gupta and Smith (1969)
Chordata			
Urochordata			
Ascidiacea tethyodea			
Stolidobranchiata			

(*continued*)

Table 6.1 (*continued*)

Description of cells/tissue	Cognomes	S^n/a (nm)	References
Golgi of test cells in the ovary of *Styela* sp.	Honeycomb, lattice-like		Kessel and Beams (1965)
Cephalchordata			
ER in Joseph's cells of the *Branchiostoma lanceolatum*	Meandrous tubules	$G^2/175$	Welsch (1968)
Vertebrata			
Agnatha; Cephalaspidomorphii			
Petromyzoniformes			
ER in retinal pigment epithelium cells of *Lampetra fluviatalis*	Undulated membrane complex	$G^4/155$	Öhman (1974)
Osteichthyes			
Actinopterygii			
Salmoniformes			
ER in epithelium of the olfactory organ in *Salmo trutta trutta*	Turtuous interconnected ER		Bertmar (1972)
Plasma membrane in gill epithelia cells of *Salmo salar*	Tubular system	D	Pisam *et al.* (1995)
ER in adrenocortical cells of *Salmo fario*	Imbricated cisternae of ER	$G^2/200$	Jung *et al.* (1981)
Siluriformes			
ER of clear cells in the dendritic organ of *Plotsus anguillaris*	Tubular network	D/100	van Lennep and Lanzing (1967)
Anguilliformes			
ER in "club cells" of juvenile *Anguilla rostrata*	Array of circular figures		Leonard and Summers (1976)

Perciformes			
ER in chloride cell of freshwater-adapted *Scophthalmus maximus*	Membraneous tubular system	D	Pisam *et al.* (1990)
Plasma membrane in gill epithelia cells of *Oreochromis niloticus*	Tubular system	D	Pisam *et al.* (1995)
Dipnoi			
Lepidosireniformes			
ER of Neuroepithelial cell in the lung of *Protopterus aethiopicus*	Paracrystalline inclusion		Adriaensen *et al.* (1990)
Crossopterygii			
ER in retinal pigment epithelium cells of *Latimeria chalumnae*	Regular arrays of tubules	G	Locket (1973)
Amphibia			
Anura			
Pipidae			
Mitochondria in Sertoli cells of *Xenopus laevis*	Regularly fenestrated cristae	$D^2/105$	Kalt (1974)
Discglossidae			
ER in intestinal epithelium cells of *Alytes obstetricans*	Sinusoidal tubules		Hourdry (1969)
Ranidae			
ER in secretory gland of *Dendrobatidae anthony*, *D. auratus*	Crystalloid	G	Neuwirth *et al.* (1979)
Urodel			
Salamandridae			
ER in oocyte of *Necturus maculosus maculosus*	Annulate lamellae		Kessel (1990)
ER in retinal pigment epithelium cells of *Notophtalamus viridescens*	Fenestrated lamellae		Yorke and Dickson (1985)

(*continued*)

Table 6.1 (*continued*)

Description of cells/tissue	Cognomes	S^n/a (nm)	References
Bufonidae			
ER of cells in the parotoid gland of *Bufo alvarius*	Crystalloid		Cannon and Hostetler (1976)
ER in spermatids of *Bufo arenarum*	Annulate lamellae		Cavicchia and Moviglia (1982)
Reptilia			
Lepidosauria			
Squamta			
ER in spermatids in *Anolis carolinensis*	Membranous body		Clark (1967)
Aves			
Galliformes			
ER in retinal pigment epithelia cells of *Cortunix cortunix japonica*			Ahn (1971)
ER of epithelium in uropygial gland of *Cortunix cortunix japonica*	Crystaloid		Fringes and Gorgas (1993)
Mammalia			
Scandentia			
Tupaiidae			
Mitochondrias in photoreceptor cone cell of *Tupaia glis*	Concentric whorls of cristae	$G^{10}/500$	Samorajski *et al.* (1966)
SER of cells in the adrenal cortex *T. glis*	Crystalloid	D	Hostetler *et al.* (1976)
Mitochondria in retinal cone cell of *Tupaia belangeri*	Peculiar whorls of cristae	$G^{12}/400$	Foelix *et al.* (1987), Knabe and Kuhn (1996), Knabe *et al.* (1997)
Chiroptera			
Molossidae			
ER of cells in sebaceous gland of *Tadarida brasiliensis*	Crystalloid	$D^2/105$	Gutierrez and Aoki (1973)

Carnivora			
Felidae			
ER of bright columnar cells in the vomeronasal organ of the cat	Hexagonal crystal-like membrane	G	Seifert (1971, 1972, 1973)
Canidae			
ER of follicular cells in adenohypophysis of the dog	(Tweedlike) paracrystal		Nunez and Gershon (1981)
ER in cutaneous histiocytoma cells of the dog	Paracrystal		Marchal *et al.* (1995)
ER in adventitial cells of the dog	Tubular aggregates		Blinzinger *et al.* (1972)
ER in mononuclear cells of dog treated with anti-dog-lymphocyte serum	Inclusion body surrounded by limiting membrane		Somogyi *et al.* (1971)
Lagomorpha			
Leproidae			
ER in ovarian steroid cells of the rabbit			Blanchette (1966a, b)
ER of type II cells in taste buds of male albino rabbit			Toyoshima and Tandler (1987)
ER in endothelial cells and macrophage of the New Zealand white rabbit infected with herpes simplex virus	Crystalline aggregates		Baringer and Griffith (1970)
Ochotonidae			
ER in Müller cell of *Ochotona* sp.	Well-developed networks of ER	$G^2/315$	Hirosawa (1992)
Artiodactyla			
Suidae			
ER in skin cells of pig infected with swine pox virus	Cytoplasmic inclusion		Cheville (1966)

(*continued*)

Table 6.1 (*continued*)

Description of cells/tissue	Cognomes	S^n/a (nm)	References
ER in endothelial cells of cervical cord of the pig infected with virus	Crystal arrays		Koestner *et al.* (1966)
Bovidae			
ER of cell in preputial gland of female *Capricornus cripus*	Grids of SER	G/80	Atoji *et al.* (1989)
Intranuclear tubules in bovine tissue with papulosa-virus infection	Intranuclear tubule-like structure		Pospischil and Bachmann (1980)
Perissodactyla			
Equidae			
ER in sebaceous gland of Equidae	Grids of SER	G	Jenkinson *et al.* (1985)
Rodentia			
Muridae			
ER in rat renal tubule cells	Fenestrated membranes		Bergeron and Thiéry (1981)
ER in rat hepatocytes after hexachlorohexahydrophenanthrene in diet	Flattened vesicles		Norback and Allen (1969)
ER in hepatocytes of carbon tetrachloride fed rats	Labyrinth tubular aggregates		Reynolds and Ree (1971)
ER in rat hepatocytes after phenobarbital treatment	Meshed network		Bolender and Weibel (1973)
ER in hepatomas of the rat			Hruban *et al.* (1972)
ER in lutein cells of the rat after cycloheximide treatment	Crystalline tubular aggregates		Horvath *et al.* (1973)
ER in adrenal medullary cell of chlophentermine treated rat	Crystalloid body		Lüllmann-Rauch and Reil (1973)
ER in adrenal cortical cell of chlophentermine treated rat	Dense body		Lüllmann-Rauch and Reil (1973)
ER in meibomian glands of the rat			Sisson and Fahrenbach (1967)
Mitochondria in skeletal muscle of the rat			Leeson and Leeson (1969)

ER in jejunal absorptive cells of rat intestine			Hatae (1990)
ER in vomeronasal epithelium in the rat	Membranous body		Garrosa and Coca (1991)
ER in cell of sebaceous gland in mouse skin	Crowded elements		Rowden (1968)
ER of neurons in the mice	Interconnected segments of SER		Johnson *et al.* (1975)
ER in testicular interstitial cells of mice	Network of tubules		Christensen and Fawcett (1966)
ER in Leydig cells of mice	Tubular profiles		Russel and Burguet (1977)
ER in mice retinal pigment epithelium after mild thermal exposure	Lacy patterened ER		Kuwabara (1979)
ER in hepatocytes of chlophentermine treated mice	Crystalline-like body		Lüllmann-Rauch and Reil (1973)
ER in hepatocytes of mice infected with mouse hepatitis virus	Peculiar tubular structures		Ruebner *et al.* (1967)
ER in mice brain cells inoculated with St. Louis encephalitis virus	Convoluted membranous mass		Murphy *et al.* (1968)
ER in neuron of suckling mouse infected with Semliki Forest virus	Anastomosing membrane tubules		Grimley and Demsey (1980, p. 151)
Cricetidae			
ER in UT-1 cells with HMG-CoA reductase expression	Sinusoidal ER	$D^2/245$	Pathak *et al.* (1986)
ER of CHO cells with rubella virus E1 glycoprotein expression	Tubular membrane		Hobman *et al.* (1992)
ER in hepatocytes of the hamster after phenobarbitone treatment	Membrane complex		Ghadially (1988, p. 512)
ER in sebaceous gland of the hamster	Grid of SER		Bell (1974a)

(*continued*)

Table 6.1 (*continued*)

Description of cells/tissue	Cognomes	S^n/a (nm)	References
ER in sebaceous gland of androgen treated hamster	Grids of SER		Bell (1974b)
ER in smooth muscle cell of triparanol treated male hamster	Dense bodies		Chen and Yates (1967)
Mitochondria in serous secretory cells of *Meriones unguiculates*		P^2/175	Spicer *et al.* (1990)
Subdermal tumour in the hamster produced by inoculation of: M-1	Undulating tubules, UMS		Chandra (1968)
Caviidae			
ER in adrenal cortical cells of fetal guinea pig, *Cavia* sp.			Black (1972)
ER in receptor cells in the vomeronasal organ of newborn *Cavia* sp.			Mendoza and Kühnel (1989)
Primates			
Strepsirhini (Prosimii)			
ER in sebaceous gland of *Galago senegalensis*	Tubules of SER	G, P	Bell (1974a)
ER of interstitial cells in the antebrachial organ of *Lemur catta*	Crystalloid	G/70	Sission and Fahrenbach (1967)
Haplorihini			
Tarsiiformes			
ER in sebaceous gland of *Tarsier syrichta*	Grids of SER	D^2	Bell (1974a)
Simiifomes			
Cerchopithecidae: ER in CV-1 cells infected with simian virus 40	Tubular membranes network		Kartenbeck *et al.* (1989)
ER in COS cells upon overexpression of msALDH	Crystalloid		Yamamoto *et al.* (1996)
ER in COS-7 and CV-1 cells upon overexpression of cytochrome b(5)	Organized SER	G^2, D^2	Snapp *et al.* (2003)

	ER in Vero cells infected with SARS coronavirus	Tubuloreticular structures	G	Goldsmith *et al.* (2004)
	ER in sinusoidal endothelial cell in liver of Macaca fascicularis	Crystalloids		Tanuma (1983)
Mulatta:	ER in sebaceous gland of *Macaca menstrina*	Tubules of SER		Bell (1974a,b)
	ER in retinal epithelium cells of *Macaca mulatta*	Peculiar body		Ishikawa (1963)
	ER in endothelial cells of the glomerular capillaries in *M. Mulatta*	Round of hexagonal bodies		de Martino *et al.* (1969)
	ER in endothelial cells in liver of *M. mulatta*	Cytoplasmic crystalloid		Ruebner *et al.* (1969)
	Ibidem with nutritional cirrhosis	Cytoplasmic crystalloid		Ruebner *et al.* (1969)
	ER in epidermal pox disease of *M. mulatta*	Crystalloid		Casey *et al.* (1967)
	ER in spinal/endothelia cells of *M. mulatta* after tumor induced by sarcoma virus	Crystalline inclusion		Munroe *et al.* (1964)
	ER in kidney cells of *M. mulatta* infected with Tana poxvirus	Honeycombed crystals		España *et al.* (1971)
	ER in macrophages, neutrophilic granulocytes and plasma cells of *M. mulatta* infected with SIV	Tubuloreticular structures		Kaup *et al.* (2005)
	ER in monkey kidney CMK cells infected with poliovirus	Paracrystalline arrays		Hashimoto *et al.* (1984)
	ER in endothelial cells of monkey spinal cord infected with poliovirus	Paracrystalline arrays		Blinzinger *et al.* (1969)
	ER in MA 104 cells infected with Simian rotavirus SA11	Smooth membrane vesicles		Quan and Doane (1983)
	ER in LLC-MK_2 infected with rubella virus	Crystal lattice-like structure		Kim and Boatman (1967)

(*continued*)

Table 6.1 (*continued*)

Description of cells/tissue	Cognomes	S^n/a (nm)	References
Ceboidea: ER in rous sarcoma virus induced tumour cells of Saquinus sp.	Membrane inclusion	P^2/175-220	Smith and Deinhardt (1968)
Hominoiddea: ER in hepatocytes of δ-agent inoculated Pan trodeglytes			Canese *et al.* (1984)
ER in hepatocytes of P. trodeglytes post experimental hepatitis	UMS		Pfeifer *et al.* (1980)
ER in endothelial cells of human and chimpanzee liver infected with hepatitis virus	Tubuloreticular and paracrystalline inclusion		Schaff *et al.* (1992)
Man: ER in villus absorptive cells in fetal small intestine of man	Convoluted membrane		Moxey and Trier (1979)
ER in cells of adrenal gland in man			McNutt and Jones (1970)
ER in HEp-2 cells infected with Ilheus virus	Knotted membranes		Tandler *et al.* (1973)
ER in human cancer cell lines: F-3, -9, -24, -53, No. 2117	UMS		Chandra (1968)
ER in HeLa cells	Cotte de maillet		Franke and Scheer (1971)
ER in HT-29 cells infected with rotavirus	Tubuloreticular structures		Tinari *et al.* (1996)
ER in cells from lymph-node culture of a patient with reticulum-cell sarcoma	Membrane inclusion with crystalline pattern		Moore and Chandra (1968)
ER in B lymphocyte of a 6-month-old male infant	Tubular arrays		Geha *et al.* (1974)
ER in endothelial KS cells	Paracrystalline inclusions		Marquart (2005)
ER in P3-J cells	UMS		Chandra and Stefani (1976)
ER in human lymphocytes	Microtrabecular lattice		Guatelli *et al.* (1982)
Mitochondria in adenoma of submandibular gland of man	Reticulate cristae		Tandler and Erlandson (1983)

Mitochondria in metastatic melanoma in man			Ghadially (1988, p. 212)
Lysosomes in human myxoid chondrosarcoma	Vesicular structure		Cameron *et al.* (1992)
ER in human embryonic kidney cells infected with HRV	Micro- TRS		Ghadially (1988, p. 496)
ER in epithelial lung carcinoma of man	TRS		Schaff *et al.* (1976)
Inner nuclear membrane in parosteal sarcoma of man	UMS	D	Murray *et al.* (1983)
ER in bronchiogenic carcinomas			Ghadially (1988, p. 96)
ER of endothelial cells on glomerular capillaries of nephritic man	Crystalline bodies		de Martino *et al.* (1969)
ER of endothelial cells in a hepatoblastoma of man			Gonzales-Crussim and Manz (1972)
ER in soft tissue sarcoma of man	TRS		Szakacs *et al.* (1991)

S^n/a Indicates that the membrane (surface) morphology (*S*) is consistent with (*n*) membranes or multiple (*m*) membranes with a lattice size of (*a*).
The listed unit cell size is based on either DTC analysis or direct measurements of the 2D lattice parameters. UMS: undulating membrane structure; TRS: tubuloreticular structure; PER: paracrystalline ER; SER: smooth endoplasmic reticulum.
The table summarizes the observation of cubic membranes in normal, pathological, and experimentally manipulated cells.

indicator of infection or transformation. For example, TRS have been observed in cells infected with SARS (Almsherqi *et al.*, 2005) and HIV (Kostianovsky *et al.*, 1987).

In addition to TRS, annulate lamellae (AL) are another type of convoluted 3D membrane structure, and their appearance is also often correlated with that of cubic membranes. AL are frequently observed in differentiating gamates, namely in vertebrate oocytes and in spermatogonia, and appear to occur in close association with the cell nucleus (see Table 6.1). Tangential TEM sections of AL most often exhibit a hexagonal arrangement (Kessel, 1983), whereas perpendicular sections do not reveal any obvious symmetrical arrangement, even though they always exhibit an astonishingly regular organization, indicating an underlying periodic structure. Based on the apparent morphological similarities between AL and the NE, it has been suggested that AL represent a cytoplasmic NE extension that functions as a reservoir for both ER membrane components and nuclear pores (Kessel, 1983, 1992). In favor of such speculations is the fact that AL have been observed in direct continuity with the outer nuclear membrane, and that they also have been suggested to contain nuclear pore complexes (Landh, 1996). AL are assembled of superimposed pairs of membrane bilayers, which join along the pores whose distribution may vary (hexagonal, quadratic, or random). The pores present in AL are either facing each other if the membrane symmetry is hexagonal (Fig. 6.4B) or the appearance of pores alternates in a quadratic membrane arrangement (Fig. 6.4A).

2.2. Membrane polymorphisms

The coexistence of different subtypes of cubic membranes or together with other membrane organizations within the same cell organelle is quite frequent, pointing to structural or functional relationships between these membrane arrangements (Fig. 6.4E). Probably the most evident example is the ER where different membrane morphologies such as cubic membranes, lamellar and hexagonal membranes, and whorls coexist quite commonly (Landh, 1996; Snapp *et al.*, 2003). Coexistence of at least two cubic membrane subtypes within the same organelle has also been observed in mitochondria of amoeba *Chaos carolinense* (Deng and Mieczkowski, 1998). In this organism, the relative abundance of gyroid (G) or diamond (D) and primitive (P) subtypes of cubic morphology changes during starvation, the biological significance of this polymorphic behavior, however, is currently unknown.

The ease with which cubic membranes and other membrane arrangements are interconverted can be attributed, at least in part, to the effect of weakly dimerizing ER proteins (Snapp *et al.*, 2003). Previous work suggested that crystalloid ER biogenesis entailed a tight, zipper-like dimerization of the cytoplasmic domains of certain ER-resident proteins

(Yamamoto *et al.*, 1996). However, Snapp *et al.* (2003) found that organized smooth ER (OSER)-inducing proteins can trigger cubic membrane formation upon over-expression through low-affinity interactions between cytoplasmic domains. This observation might explain phenomena such as (a) the heterogeneity of ER membrane structures, (b) the high rate of (reversible) lamellar to cubic membrane transition, and (c) the technical difficulties and limitations in isolating intact cubic membranes from biological samples.

2.3. Cubic membranes versus cubic phases

Lipidic bicontinuous cubic phases consist of hyperbolically curved bi-layers where each monolayer is draped over a periodic cubic (minimal) surface (Fig. 6.2D). With respect to bilayer arrangements, the geometries of cubic membranes are similar to those of the cubic phases, however, two major differences exist: (i) the unit cell size and (ii) the water activity. It has been argued that the latter must control the topology of the cubic membrane (Bouligand, 1990) and hence that the cubic membrane structures must be of the inverted type rather than "normal" type (type I). All known lipid–water and lipid–protein–water systems that exhibit phases in equilibrium with excess water are of the inverted type (type II). Thus, water activity alone cannot determine the topology of cubic membranes. Inverted cubic phases have been observed with very high water activity (70–90%), in the mixtures of lipids, in lipid–protein systems, in lipid–polymer systems (Landh, 1994), and in lipid and lipopolysaccharide mixtures (Brandenburg, 1990, 1992).

Most cubic phases in lipid–water systems exhibit unit cell parameters not larger than 20 nm, while in cellular cubic membranes the lattice size is usually larger than 50 nm. However, in lipid–protein–water, lipid–poloxamer–water and lipid–cationic surfactant–water systems, cubic phases with cell parameters of the order of 50 nm have also been observed (Landh, 1996). On the other hand, the unit cell size of cubic membranes is rarely less than 50 nm (e.g., in prolamellar bodies) and the size ranges from 50 to 500 nm. Cubic membranes with large lattice size (500 nm) were frequently observed in chloroplast membranes of green algae *Zygnema* (Fig. 6.6).

Additionally, cubic membranes are formed under conditions corresponding to a highly regulated multiphase "equilibrium" process. This is supported by the fact that they are usually formed in close contact with different other membrane configurations. The asymmetry of biological membranes with respect to the two leaflets is likely to affect cubic membrane formation, in particular as a consequence of lipid and protein composition, and interaction with the surrounding ion milieu.

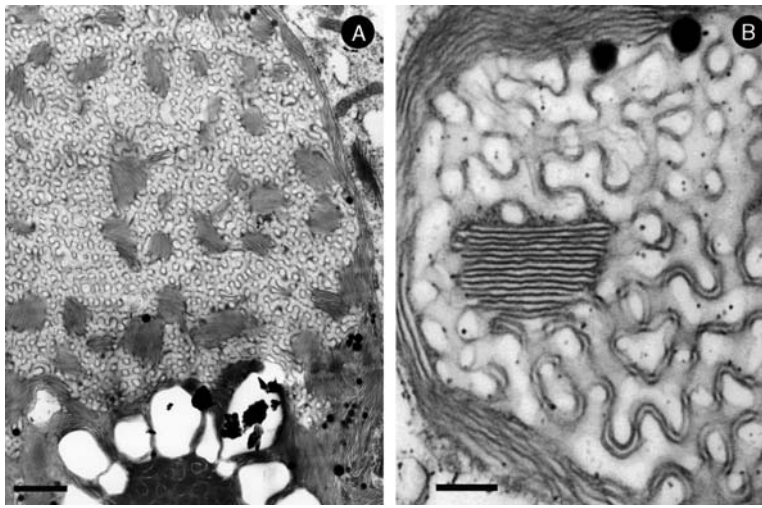

Figure 6.6 Multilayer membrane organization and transformation. (A) An overview of the ultrastructure of chloroplast membrane in green algae *Zygnema* sp. (LB923) at 41 days of culture. Scale bar: 1 μm. (B) Several subdomains display different morphologies, ranging from simple stacked lamellar in direct association with paired parallel membranes (2 membranes; upper left) and double paired parallel membranes (4 membranes; lower right) of the gyroid-based cubic membrane morphology. Scale bar: 500 nm (Deng, 1998).

2.4. Understanding membrane morphology by transmission electron microscopy

A survey of the literature (Table 6.1) immediately unveils a multitude of "unusual" membrane organizations in various cell types. Most of these depictions were obtained by TEM of chemically fixed and thin-sectioned cells and tissues. Dependent on the thickness and orientation of the section through the specimen, relative to the coordinates of an ordered 3D structure, various types of projection patterns are observed. As a consequence, membrane ultrastructures derived from TEM images are frequently misinterpreted, in particular for the highly folded and interconnected 3D morphologies resembling cubic membranes. TEM relies on 70–90 nm thick sections through the specimens and the 2D image obtained is the result of a projection of a 3D structure. Therefore, nonlamellar biological membranes, such as inverted hexagonal or cubic structures, may yield very heterogeneous projection patterns by TEM, dependent on the orientation of the section relative to the structural axes (Fig. 6.3). Interpretation of TEM membrane patterns is further complicated if the lattice size of the observed structure is considerably smaller than that of the section thickness.

Serial sections or scanning EM, as well as tilting and rotation of the sample, may facilitate structure interpretation. Furthermore, TEM of multiple randomly cut sections through a specimen provides a rather simple means to reconstruct its 3D structure. More elaborate electron tomography (ET) has contributed a great deal of resolution to understanding cubic membrane organizations and their continuity with and relations to the neighbor structures (Deng *et al.*, 1999). In ET, rather thick sections (400 nm) are imaged in multiple tilted angles (up to $\pm 60^{\circ}$), yielding a large number of projections; these images are reconstructed by computational image analysis into a 3D representation of the object, which allows the 3D reconstruction of cellular structures with a resolution of 5 nm, that is, approaching the level or larger molecular assemblies (for a review see Lucic *et al.*, 2005). EM tomography has previously been successfully applied to determine cubic membrane transition of the inner mitochondrial membrane morphology in the amoeba *C. carolinense* upon starvation (Deng *et al.*, 1999). Cryo-ET from specimens in vitreous ice further improves sample preservation and membrane resolution, but obviously is not yet routinely established. Cryo-ET avoids common artifacts of conventional EM preparation techniques and is also suited for high-resolution analyses of membrane-bound organelles (Hsieh *et al.*, 2006; Lucic *et al.*, 2005).

Most EM experiments described in the literature that focus on biological membranes were obviously not designed to depict three-dimensionally convoluted membrane arrangements. Therefore, alternative methods have to be applied to reconstruct—potential—3D membrane morphologies from single TEM sections. Indeed, based on well-defined mathematical models of cubic membrane arrangements, projections can be calculated that simulate various section orientations and thicknesses (Fig. 6.3). Such a "direct template correlative" (DTC) matching method (Almsherqi *et al.*, 2005, 2006; Deng and Mieczkowski, 1998; Landh, 1995, 1996) has been developed based on pattern and symmetry recognition. Through the DTC method, the electron density of the TEM image is correlated to a library of computer-simulated 2D projection maps that allows to unequivocally deduce the nature of the cubic membrane arrangement. An application of the DTC method to identify cubic membrane organization in TEM micrographs is shown in Fig. 6.7. In brief, the 2D projections (Fig. 6.7C) calculated from a mathematical 3D model (Fig. 6.7B) are matched with a selected TEM micrograph (Fig. 6.7A); consequently, a successful pattern match defines the nature of the membrane arrangement in 3D (Deng and Mieczkowski, 1998; Landh, 1995, 1996). The DTC method simplifies the experimental requirements for recording cubic membranes in biological samples, and can also be applied to examine published TEM micrographs in retrospect. The following section highlights the identification of cubic membrane structures in multiple cellular systems and subcellular organelles.

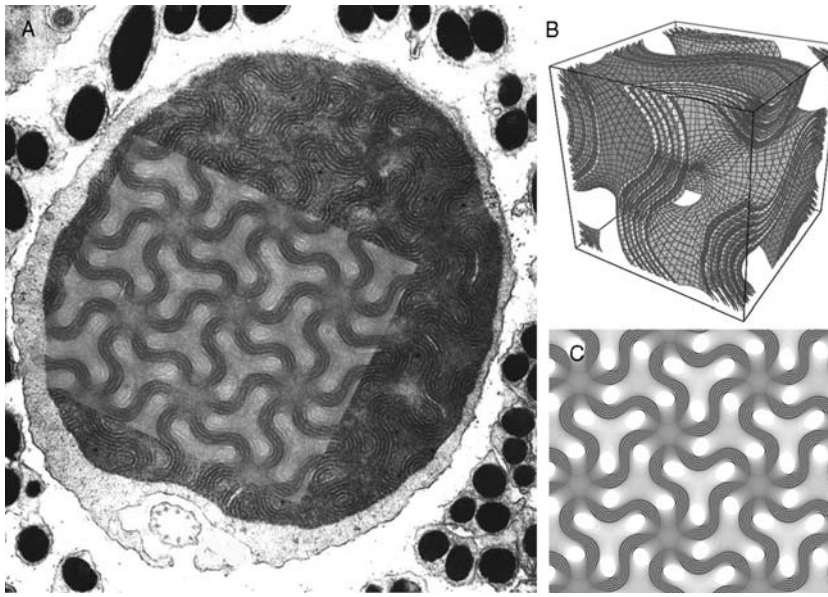

Figure 6.7 Direct template matching method. (A) TEM micrograph of lens mitochondria observed in the retinal cones of tree shrew species; (B) 6 pairs (12 layers) of G-based parallel level surfaces—a mathematical 3D model—that can be used to describe G type of cubic membrane morphology and the corresponding computer-simulated 2D projection map (C) derived from the corresponding 3D model in (B) (image provided by Prof. S. Wagon, St. Paul, Minnesota); TEM micrograph of lens mitochondria (A) perfectly match the theoretical projection (C), that is generated from 6 pairs (or 12 layers) of G-level surfaces (± 0.1, ± 0.2, ± 0.4, ± 0.5, ± 0.7, ± 0.8) with a quarter of a unit cell section thickness viewed from the lattice direction [1, 1, 1]. Note the matching details of the TEM projection and computer-simulated 2D projection such as the appearance of density of the lines (membranes) and the density between the sinusoid membranes. The original TEM micrograph in (A) is adopted from Fig. 6.10, from Foelix *et al*. (1997) with kind permission of Springer Science and Business Media. (14,000 ×).

3. Cubic Membranes in Nature

3.1. Cubic membranes: From protozoa to mammals

Extensive membrane proliferations leading to unusual and highly convoluted depictions in TEM micrographs have been observed in numerous cell types from all kingdoms of life and in virtually any membrane-bound subcellular organelles, as outlined above. Table 6.1 summarizes a survey of the literature of the past six decades on cubic membrane morphologies identified in organelles, from protozoan to human cells. The occurrence of cubic membranes is listed by genera and, if applicable, the type and lattice size of the cubic membrane extracted from the published

TEM images are presented (see also Hyde *et al.*, 1996; Landh, 1996). Not surprisingly, due to the absence of a clear understanding of the 3D structure of the depicted membranes, many of the examples have been considered as novelties with little or no reflection on the wealth of related contributions in the literature. Hence, these morphologies appear under a large variety of nicknames, some of which are also listed in Table 6.1. Furthermore, the examples have been chosen to best represent the structural characteristics of cubic membranes, and an effort has been made to leave out those perhaps less recognizable structures such as ''membraneous tubular'', ''cisternal systems'', ''tubular inclusions'', or ''cisternal convolutions'' etc. In many cases where we have chosen not to classify the cubic membrane it is mainly due to the lack of discernible details in the TEM micrographs. Interestingly, many of these undetermined cubic membrane morphologies are reported in pathological conditions in hominoidae.

3.2. Organelles with cubic membrane structure

3.2.1. Endoplasmic reticulum

The ER was found to be the most prominent target of morphological alterations because of its highly convoluted and dynamic structure and crucial functions in membrane lipid synthesis and assembly, protein synthesis and secretion, ion homeostasis, and membrane quality control. These morphologies appear under numerous nicknames in the literature, such as ''undulating membranes'' (Schaff *et al.*, 1976), ''cotte de mailles'' (Franke and Scheer, 1971), ''membrane lattice'' (Linder and Staehelin, 1980), ''crystalloid membranes'' (Yamamoto *et al.*, 1996), ''paracrystalline ER'' (Wolf and Motzko, 1995), ''tubuloreticular structures (TRS)'' (Grimley and Schaff, 1976), and recently, as OSER (Snapp *et al.*, 2003).

Periodic symmetrical transitions of the ER are usually correlated with overexpression of certain ER-resident membrane proteins (Table 6.2) (see below). For example, overexpression of HMG-CoA reductase isozymes induces assembly of nuclear and cortical ER stacks with 2D symmetry, termed ''karmellae'' in yeast (Profant *et al.*, 2000; Wright *et al.*, 1988). Overexpression of this enzyme in UT-1 (Chin *et al.*, 1982) or Chinese Hamster Ovary (CHO) cells (Jingami *et al.*, 1987; Roitelman *et al.*, 1992) induces formation of crystalloid ER, which houses most of the HMG-CoA reductase enzyme (Anderson *et al.*, 1983; Orci *et al.*, 1984). This correlation may imply a specific structure–function relationship of cubic membrane formation as a consequence of an altered protein or lipid inventory of the membrane.

The cells of the phloem in plants are involved in the long-distance transport of nutrients and are known as sieve elements. Interestingly, the ER of differentiating sieve elements is a rare example in Nature in which

Table 6.2 Occurrence of crystalloid ER membranes in cell lines overexpressing certain ER-resident membrane proteins

Description of cells/tissue	Overexpressed proteins	Cognomes	Membrane organization	References
UT-1 cells (Compactin resistant CHO cells)	HMG-CoA reductase	Crystalloid ER	Hexagonal, cubic (G^2)	Chin *et al.* (1982); Anderson *et al.* (1983); Pathak *et al.* (1986); Kochevar and Anderson (1987); Orci *et al.* (1984)
CHO cells	HMG-CoA reductase	Crystalloid ER	Hexagonal	Jingami *et al.* (1987)
Yeast	HMG-CoA reductase	Karmellae	Multilayer lamellar	Wright *et al.* (1988)
Yeast	Cytochrome b(5)	Karmellae	Multilayer lamellar	Vergères *et al.* (1993)
CV-1, COS-7	Cytochrome b(5)	Organized SER	Multilayer lamellar (whorls), cubic (D^2, G^2)	Snapp *et al.* (2003)
COS-1 cells	msALDH	Crystalloid ER	Cubic (G)	Yamamoto *et al.* (1996)
COS cells	$InsP_3$ receptor	Cisternal stacks	Multilayer lamellar, whorls	Takei *et al.* (1994)
CHO cells	Unassembled rubella virus E1 glycoprotein subunits	Tubular network	Retiform	Hobman *et al.* (1992)
HEK293 cells/ human	Cytochrome P450 2B1	Crystalloid ER	Hexagonal	Sandig *et al.* (1999)
Escherichia coli	Subunit (b) of F1F0 ATP synthase	Intracellular membrane	Hexagonal	Arechaga *et al.* (2000); Gales *et al.* (2002)
E. coli	Fumarate reductase	Tubule	Hexagonal	Weiner *et al.* (1984)

two cubic membranes with the same structure but with different unit cell parameters, may coexist in the same cell (Behnke, 1965, 1968; Landh, 1996). These cells lack a nucleus and the cytoplasmic connection and exchange between vertically stacked cells is enabled through the perforated walls of the sieve elements (Behnke, 1965). Their function is to transfer the products of photosynthesis from the manufacturing site (leaves) to the storage cells (stem, roots, and seeds). The different types of cubic membranes may perhaps facilitate transport of various materials at different rates within the same cell.

3.2.2. Inner mitochondrial membranes

Numerous researchers have reported mitochondria with inner membrane configurations that resemble cubic membrane morphologies (Brandt and Pappas, 1959; Kalt, 1974; Tahmisian *et al.*, 1956). Possibly the best-characterized cubic membrane transition was observed in the mitochondrial inner membranes of the free-living giant amoeba, *C. carolinense* (Deng and Mieczkowski, 1998). In this organism, mitochondrial inner membranes undergo dramatic changes in 3D organization upon food depletion, providing an attractive, reversible model system to investigate induced membrane reorganization. Within one day of starvation, 70% of mitochondria undergo this morphological transition, which is observed in virtually all mitochondria after 7 days of starvation (Daniels and Breyer, 1968). This structural alteration of mitochondria in *C. carolinense* has been identified by a number of laboratories; however, in several reports the inner mitochondrial membranes take the appearance of tubular-like configurations that may appear in conjunction with well defined cubic membranes (Borysko and Roslansky, 1959; Brandt and Pappas, 1959; Daniels and Breyer, 1968; Sedar and Rudzinska, 1956). Indeed, by EM tomography, we have unambiguously demonstrated that inner mitochondrial membranes in *C. carolinense* cells adopt cubic morphology under starvation conditions (Deng *et al.*, 1999). This induced transition is accompanied by alterations in cellular oxidative stress response, which led us to speculate that cubic membrane formation may be associated with oxidative stress (Deng *et al.*, 2002) (see also discussion below). Intriguingly, formation of cubic membranes in amoeba *Chaos* is fully reversible to wild-type tubular morphology, upon refeeding (Deng and Mieczkowski, 1998).

A similar cubic architecture of inner mitochondrial membranes was identified in a TEM ultrastructural study (Kalt, 1974) that describes mitochondrial pleomorphism in supporting (sustentacular) cells in testis of African clawed frog, *Xenopus laevis*. The mitochondrial membrane constellation in the mature stage of Sertoli sustentacular cells exhibits the D subtype of cubic membrane morphology.

The mitochondria in the inner segment of the retinal cones of tree shrew species, *Scandentia*, the common tree shrew (*Tupaia glis*), and the northern

tree shrew (*Tupaia belangeri*) (Foelix *et al.*, 1987; Knabe and Kuhn, 1996; Knabe *et al.*, 1997) are unique in size and ultrastructural arrangement of their inner membranes (Samorajski *et al.*, 1966). These unusually large, patterned mitochondria exhibit one of the most complicated cubic membrane architectures known to date, with the highest possible symmetry (G subtype) of up to 12 layers of three-dimensionally folded membranes (see discussion below) (Fig. 6.7).

3.2.3. Plasma membrane

Convoluted invaginations of the plasma membrane that are associated with the "smooth spongiome," which is part of the contractile vacuole complex in *Paramecium multimicronucleatum*, have been proposed to be of the G subtype of cubic membrane organization (Allen, 2000; Landh, 1996; Patterson, 1980). *Paramecium* cells are able to maintain an almost constant intracellular osmolarity regardless of the environmental osmolarity. The complex regulation of the cell volume and osmotic gradient is primarily established by the smooth spongiome, which exhibits cubic membrane organization. Therefore, cubic membranes have been suggested to play roles in water segregation and intracellular volume and osmolarity control (Landh, 1996).

"Honeycomb" structures of the T-tubular system in skeletal muscles have been observed in numerous diseased as well as in experimentally induced cases. Such structures were shown to be in continuity with the extra-cellular space and can thus be regarded as extensions of plasma membrane invaginations. The significance of honeycomb t-tubules is, however, unknown (Mastaglia and Walton, 1992), and surprisingly few studies deal with their 3D organization. Despite the elegant study of Ishikawa (1968), the 3D structure of these "honeycombs" was resolved only 30 years after their first discovery (Landh, 1996) and unambiguously demonstrated to be of cubic membrane morphology of the gyroid (G) subtype.

3.2.4. Photosynthesis-associated cubic membranes

The structure of photosynthetic membranes and their assembly during development have been extensively studied (Gunning, 1965; Gunning and Jagoe, 1967; Gunning and Steer, 1975). In bacteria, several publications report lattice-like membrane morphologies as a variation of the more common multilamellar (thylakoid) configuration. In vegetative, photosynthetically active cyanobacteria, *Anabaena sp.*, Lang and Rae (1967) reported a "prolamellar-like lattice", which was formed through continuous foldings of the photosynthetic thylakoid membranes. This cubic membrane bears a close resemblance to the prolamellar body (PLB) in higher plants, with the important difference that PLB are formed in the absence of light, whereas

cubic membranes in *Anabaena sp.* were observed in fully illuminated cultures. The analysis of micrographs (Lang, 1965) of developing heterocysts (cells involved in nitrogen fixation) of *Anabaena azollae* clearly revealed several TEM projections of more or less developed cubic membranes (Landh, 1996). Although heterocysts lack the photosynthetic apparatus, these cubic membranes appear to arise by continuous folding of the thylakoid membranes.

3.2.4.1. Chloroplasts of green algae Zygnema In certain green algae species the chloroplast membrane(s) tend to form more complex morphologies than the simple ''lamellar-like'' structures. Chloroplasts of the green alga *Zygnema* transform to G-type cubic membrane (Fig. 6.6) during the log phase of cell culture (Deng and Landh, 1995). An analysis of previously reported electron micrographs by McLean and Pessoney (1970), which described ''lamellar lattices'' in *Zygnema* chloroplasts, indeed revealed a primitive (P) subtype of cubic membrane (Landh, 1996). This particular structure represents a continuous cubic membrane organization that is composed of several, mostly parallel, lipid bilayers (Deng, 1998).

3.2.4.2. Prolamellar body The fine structure of the PLB has been extensively studied by electron microscopy (Gunning, 1965; Gunning and Jagoe, 1967; Gunning and Steer, 1975; Israelachvili and Wolfe, 1980; Menke, 1962, 1963; Murakami *et al.*, 1985; Osumi *et al.*, 1984; Wehrmeyer, 1965a, b,c). Three basic space-lattice structures of the PLB have been proposed: (i) a primitive cubic lattice in which the fundamental unit is a hexapode (Granick, 1961; Gunning, 1965; Gunning and Jagoe, 1967), (ii) a diamond-based face-centered cubic lattice in which the fundamental unit is a tetrapode (Gunning and Steer, 1975; Murakami *et al.*, 1985; Osumi *et al.*, 1984; Wehrmeyer, 1965b), and (iii) a hexagonal Wurtzite-type of lattice (Ikeda, 1968; Wehrmeyer, 1965c; Weier and Brown, 1970). The double diamond-type cubic lattice is presumably the most common cubic structure of the PLB (Landh, 1996).

3.2.5. Inner nuclear membrane

The formation of cubic membranes in the NE is not confined to the cytoplasmic side (i.e., the nuclear ER), but may also occur at intranuclear sites. This may appear surprising, however, formation of cubic membranes within nuclei could be realized by invaginations of a proliferating inner nuclear membrane. Intranuclear cubic or tubular membrane organizations usually develop in fast replicating neoplastic (tumor) cells (Babai *et al.*, 1969; Karasaki, 1970) or non-neoplastic cells such as oocytes (Kessel and Beams, 1968; Miller, 1966). Their presence might play a role in mitotic activity or in facilitating nuclear-cytoplasmic communication. In human cells, intranuclear tubular (hexagonal or cubic) membrane organization was demonstrated in the endometrium during the secretory phase of the menstrual

cycle (Bourgeois and Hubert, 1988; Ghadially, 1988). Progesterone and medroxyprogesterone can induce tubular structure formation in human endometrium (Kohorn *et al.*, 1972), which suggests a role of an extrinsic hormonal factor in cell membrane organization.

4. Biogenesis of Cubic Membranes

An extensive review of the literature reveals that virtually all membranes are capable of forming cubic structures. Their origin thus seems to be strongly coupled to the mechanisms of membrane biogenesis in general and, therefore, cubic membranes are to be considered as a defined configuration of cytomembranes. The formation and growth of cubic membranes may be a selective process to fulfill a specialized purpose under ever changing intracellular conditions. Thus, understanding the underlying rules(s) for the physiological selection between the different membrane morphologies is key. It is now well established that proteins may induce phase transition in lipid membranes resulting in new structures not observed in pure lipid–water systems (Bouligand, 1990). However, in principle, any amphiphilic molecule may be able to induce cubic membrane structures. Depending on the structure and nature of the proteins, their interactions with lipid bilayers can be manifested in very different ways. On the other hand, evidence from *in vitro* studies clearly differentiates membrane-forming lipids for their propensity to form nonlamellar structures, according to the molecular shape concept. The important structural role of membrane lipids in promoting cubic membrane formation *in vivo* is undisputed; however, only very recent evidence obtained from amoeba *Chaos* cells has correlated specific alterations of membrane lipids to cubic membrane formation *in vivo* (Deng *et al.*, submitted). Although lipids extracted from these cells may assemble to cubic phases also *in vitro* (Fig. 6.8), marked differences in lattice size clearly indicate that additional factors—presumably proteins—exist *in vivo* that determine the overall 3D appearance of these structures. Induction of cubic membranes in *Chaos* cells upon starvation represents one rare example to experimentally address the molecular mechanisms leading to their formation in the biological context.

From a topological point of view, cubic membranes appear to be formed from a structural ''template'' (the precursor of a cubic membrane), such as invaginations of a membrane. After initiation, further accumulation of membrane lipids may lead to intersection-free highly convoluted invaginations. During the folding process, the membrane must remain a continuous fluid structure that grows and interconnects without losing its polarity and integrity. Thus, the topology of the cubic membrane depends on the topology of its precursor structure. If one isolated invagination process

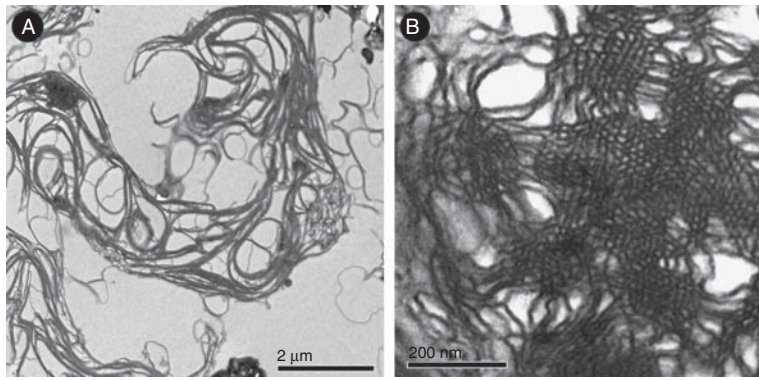

Figure 6.8 Lipid dispersion prepared from amoeba lipids (Deng, unpublished). TEM images of liposomes derived from lipids extracted from fed and 7d starved *Chaos* cells. (A) Multilamellar or whorl-like structures generated from fed cell lipids with numerous randomly distributed tubular structures, but without higher order phases. In contrast, (B) TEM data of lipid dispersion generated from lipids that were isolated from 7d starved amoeba cells show highly ordered domains.

triggers the membrane folding process, the topology will be that of a sphere, as is the case for vesicle formation during endocytosis or secretion. If more than one invagination takes place, it requires points of fusion to achieve a three-dimensionally interconnected membrane. Perhaps it is this symmetry that is the driving force for fusion; if fusion did not occur one would expect several independent cubic membrane systems to form, which would not necessarily bear any spatio-temporal correlation between each other or the periodicity of the template.

4.1. Role of membrane-resident proteins in cubic membrane formation

Cubic membrane formation is frequently associated with the overexpression of certain ER-resident proteins and, to a lesser extent, with overexpression of some inner mitochondrial membrane proteins. Table 6.2 lists major membrane proteins that have been shown to induce cubic membrane formation upon experimental dys-regulation.

4.1.1. ER proteins

HMG-CoA reductase is an ER-resident protein that is anchored to the membrane by seven membrane-spanning domains in its N-terminal part and has its catalytic domain extending to the cytoplasmic side. Elevated expression of HMG-CoA reductase is often associated with structural membrane alterations. The transmembrane region is indeed required to form crystalloid membrane structures of hexagonal (Fig. 6.5D) or cubic

(Fig. 6.5C) morphologies, upon overexpression. Deletion of two of the seven membrane spanning regions or a truncated protein did not result in crystalloid ER formation, and the protein localized to disordered sheets rather than packed membrane tubules under these conditions. High expression levels of the soluble fragment of HMG-CoA reductase did not induce any crystalloid ER, again indicating that it is the transmembrane domain of HMG-CoA reductase that plays an important role in determining the structure of crystalloid ER (Jingami *et al.*, 1987; Yamamoto *et al.*, 1996).

Crystalloid ER is frequently observed in CHO cells upon overexpression of the HMG-CoA reductase gene, or in UT-1 cells, which are a mutant variant of CHO cells that overexpress this gene by 500 fold (Fig. 6.5; Chin *et al.*, 1982). Notably, despite the presence of elevated levels of HMG-CoA reductase, which is the key enzyme of sterol biosynthesis, the membrane of the crystalloid ER appears to have very little cholesterol. Upon addition of cholesterol to UT-1 cells, which intercalates into the ER membrane, HMG-CoA reductase was subsequently degraded and the crystalloid ER disappeared (Jingami *et. al.*, 1987); sterol supplementation drastically reduced the rate of HMG-CoA reductase synthesis and also prevented the formation of new crystalloid ER. It was therefore speculated that the cubic membrane is an alteration in the feedback control of cholesterol synthesis, for the production of sterols and the biogenesis of smooth ER. Interestingly, administration of compactin, which is an HMG-CoA reductase inhibitor, also leads to HMG-CoA reductase overexpression, and induces the formation of stacked and aggregated structures, which were termed ''karmellae'' in yeast (Wright *et al.*, 1988).

The expression of msALDH in COS-1 cells also leads to alterations of the ER structure. Both HMG-CoA reductase and msALDH proteins possess large domains exposed on the cytoplasmic surface of the ER membrane, similar to the ER-resident protein, cytochrome P450. This led to the hypothesis that the formation of crystalloid membranes may require the expression of ER-resident proteins with large cytoplasmic domains (Sandig *et al.*, 1999; Snapp *et al.*, 2003; Yamamoto *et al.*, 1996).

Overexpression of specific ER-resident proteins such as cytochrome b (5) in COS-7 cells also triggers the formation of ''whorls and crystalloid OSER structures'' (Snapp *et al.*, 2003). It was proposed that the biogenesis of OSER structures involves weak homotypic interactions between cytoplasmic domains of proteins and may underlie the formation of other stacked membrane structures within the cells as well. Time-lapse imaging of OSER biogenesis revealed that these structures formed rather quickly once a threshold level of OSER-inducing proteins was exceeded; OSER-formation also involved gross remodeling of surrounding tubular ER.

In this system, the attachment to the cytoplasmic domain of different ER-resident membrane proteins of green fluorescent protein (GFP) that is capable of low affinity, head-to-tail dimerization was sufficient to induce OSER formation upon overexpression in living cells. Homotypic low affinity interactions between cytoplasmic domains of proteins thus can differentiate tubular ER into stacked lamellae or crystalloid structures; such a mechanism may underlie the reorganization of other organelles into stacked structures as well (Snapp *et al.*, 2003), and provides an intriguing model system to investigate the cellular and molecular requirements for cubic membrane formation.

4.1.2. Mitochondrial proteins

Only a few mitochondrial proteins have been reported to induce and maintain tubular inner membrane morphology upon overexpression (Mannella, 2006), however, none of them was correlated with well-defined cubic membrane formation. Mitofilin, F1F0-ATPsynthase, and fission-fusion proteins may induce tubular or stacked lamellar and whorl-type membrane structures upon experimental overexpression. F1F0-ATPsynthase is an essential enzymatic complex of the mitochondrial inner membrane, which couples the proton electrochemical gradient generated by the respiratory chain to ATP synthesis. Various studies have shown that this complex is strongly implicated in the curvature of the inner mitochondrial membrane (reviewed by Voeltz and Prinz, 2007). Dimerization of the complex drives tubulation of the cristae (Dudkina *et al.*, 2005; Strauss *et al.*, 2008), while further oligomerization of these dimers is responsible for the formation and/or stabilization of inner membrane tubules. Mitofilin is a mitochondrial inner membrane protein, which assembles into a large multimeric protein complex. siRNA knockdown of mitofilin in HeLa cells yielded mitochondria with disorganized mitochondrial inner membranes: they failed to form tubular or vesicular cristae and appeared as intermittently fused, closely packed stacks of membrane sheets, resulting in a complex maze of membraneous networks (John *et al.*, 2005). Mitofilin thus appears to be a key organizer of mitochondrial cristae morphology (John *et al.*, 2005). The role of mitochondrial proteins in cubic membrane formation in starved amoeba *Chaos*, which is a suitable model for analyzing reversible cubic membrane formation, is currently under investigation in the authors' laboratories.

4.1.3. Morphogenic proteins

Recently a class of membrane proteins known as morphogenic proteins was identified to shape the tubular ER in yeast and mammalian cells. These proteins are highly enriched in the tubular portions of the ER and virtually excluded from other regions. The study by Voeltz and coworkers (2006)

illustrated the role of Rtn4a/NogoA, a member of the ubiquitous reticulon protein family that share a conserved C-terminal reticulon domain. Overexpression of Rtn4a/NogoA in mammalian cells, promoted the formation of ER tubules; membrane tubule formation *in vitro*, on the other hand, was prevented by anti-Rtn4a/NogoA antibodies. Similar results were observed in the yeast *Saccharomyces cerevisiae*, in which overexpression of Rtn1 (the yeast ortholog of Rtn4a/NogoA in mammals) also enhanced tubular ER formation. Yeast mutants lacking both Yop1 (an Rtn1 paralog) and Rtn1 showed a disrupted tubular ER, underscoring the important function of these proteins in shaping membrane structures. Reticulons contain long, hydrophobic domains that are inserted into the outer leaflet of the lipid bilayer. Since the hydrophobic domains are longer than required for spanning a bilayer membrane, it is believed that they promote a hairpin-like insertion into the lipid bilayer and give the overall appearance of a wedge-like protein. Thus, a local concentration of reticulons might induce and stabilize a high, positive membrane curvature.

Although morphogenic proteins are believed to induce membrane curvature and shape spherical or tubular morphology, to date, none of them has been reported to induce highly organized membrane structures such as hexagonal or cubic membranes *in vivo*. One exception to the rule is the observation of a t-tubular system in skeletal muscles (Ishikawa, 1968), in which cubic membrane organization has been associated with caveolin-3 expression (Parton *et al.*, 1997). Caveolin is synthesized in the ER but mostly resides in certain domains of the plasma membrane. Caveolins are known to play a role in inducing and maintaining membrane curvature. Individual caveolin molecules are cotranslationally integrated into the bilayer of the ER. Similar to reticulons, caveolins form a hairpin-loop within the bilayer, and tend to form hexa- or heptamers. These oligomers may leave from the ER and are transported via the Golgi apparatus to the plasma membrane, where, by a yet unknown mechanism, they induce localized sites of membrane curvature, known as caveolae (Bauer and Pelkmans, 2006; Voeltz and Prinz, 2007).

4.2. Role of lipids in cubic membrane formation

Up to date, cubic membrane formation is mainly associated with overexpression of certain membrane-resident proteins. Although cubic phases are formed by ''nonlamellar'' lipids *in vitro*, only very few data directly correlate cubic membrane formation with cellular lipid profiles *in vivo* (Ryberg *et al.*, 1983). In this study it was shown that the molar ratio of monogalactosyl diacylglycerol to digalactosyl diacylglycerol was higher in the PLB fraction that exhibits cubic membrane morphology, than in the prothylakoid fraction. Also, the content of glycolipids and protochlorophyllides was increased in the PLB fraction (Ryberg *et al.*, 1983).

Lipid analyses of fed and starved amoeba (*C. carolinense*) recently performed in the authors' laboratory (Deng *et al.*, submitted) may provide a first clue towards understanding the role of membrane lipids in determining cell membrane architecture. Detailed lipid analysis of amoeba *Chaos* exhibiting cubic membrane organization in their mitochondria, revealed an unusually high concentration of highly polyunsaturated fatty acids (C22:5; docosapentaenoic acid, DPA). Three predominant lipid species, namely plasmalogen PE (C16:0p/C22:5), plasmalogen PC (C16:0p/C22:5), and diacyl-PI (C22:5/C22:5), were identified in amoeba *Chaos* lipid extracts (Fig. 6.9), and their relative amounts increased up to 2.5-fold under starvation stress conditions (Deng *et al.*, submitted). A rich body of data (for review see Nagan and Zoeller, 2001) suggests that plasmalogens—which are also present in mammalian cell membranes—may serve as mediators of membrane dynamics due to their high propensity to form inverted hexagonal structures. This property has also suggested a potential role for plasmalogens in facilitating membrane fusion processes (for review see Brites *et al.*, 2004). Biophysical studies have also shown that the presence of plasmalogen PE lowers the lamellar to hexagonal-phase transition temperature (Lohner, 1996). Interestingly, CHO cells, which display massive membrane rearrangements upon HMG-CoA reductase overexpression (Fig. 6.5), are also rich

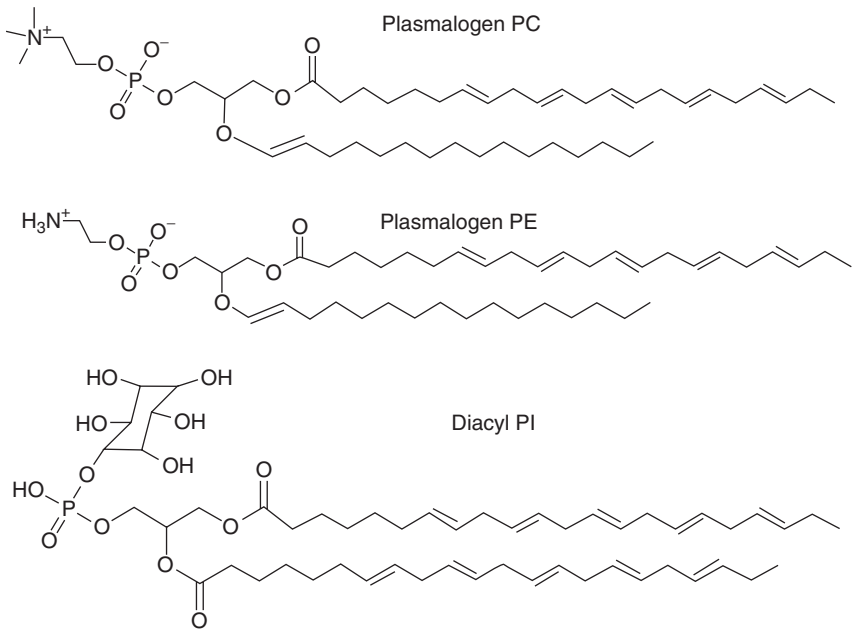

Figure 6.9 Chemical structures of three major lipids found in membrane lipids extracted from amoeba *C. carolinense*: plasmologen PC (16:0p/22:5), plasmologen PE (16:0p/22:5), and diacyl PI (22:5/22:5).

in plasmalogen lipids (up to 11% of their total phospholipids), especially plasmalogen PE (Nagan *et al.*, 1998).

4.3. Electrostatic effects on cubic membrane organization

The observation that weak molecular interactions, for example, by membrane proteins, may lead to cubic membrane transformation also suggests that electrostatic interactions play an important role in that process (Masum *et al.*, 2005, Snapp *et al.*, 2003). In a recent experimental study on the effects of divalent cations in the isolation buffers for mitochondria, we were able to demonstrate that the presence of EDTA up to 10 mM preserved mitochondrial cubic membranes *in vitro* (Fig. 6.10) (manuscript in preparation). Thus, pH and the nature of the electrolytes in the cellular milieu are likely to be important factors affecting cubic membrane morphology and integrity.

In vitro studies using monoolein membranes containing negatively-charged dioleoylphosphatidic acid have shown that the electrostatic interactions caused by surface charge of the membranes (Li *et al.*, 2001), charged short peptides such as poly-L-lysine (Masum *et al.*, 2005), Ca^{2+} concentration (Awad *et al.*, 2005), and low pH (Okamoto *et al.*, 2008) play an important role in the phase transition between lamellar and cubic phases as well as on the stability of cubic phases. As a consequence of altered electrostatic interactions at the membrane interface, induced either by the

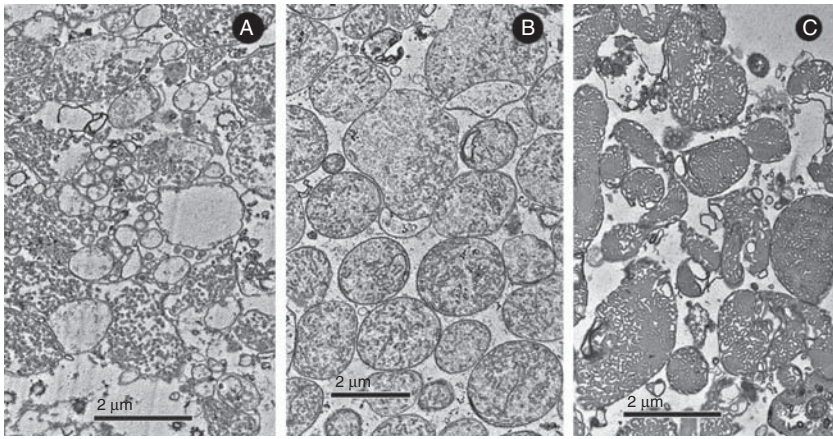

Figure 6.10 Electrostatic effects on cubic membrane organization (Deng, unpublished). Mitochondria of amoeba *Chaos* exhibiting cubic membrane arrangements were isolated in a buffer media containing (A) 50 μM, (B) 1 mM, or (C) 10 mM EDTA. Increasing the concentration of EDTA stabilized mitochondria with cubic morphology, suggesting a modulatory function of divalent cations in cubic membrane formation.

increase in surface charge density of the membrane or by a decrease in salt concentration, the lipid membrane phase may change from the lamellar to the cubic phase. Such cubic phases may not only form to adopt the altered membrane proteins or charge distribution, but may also provide the means to rapidly adjust cellular physiology to the changing environmental conditions, such as fluctuations of (local) intracellular Ca^{2+} levels. The "breathing" of cubic membranes, that is, the changes in lattice size as demonstrated *in vitro* (de Campo *et al.*, 2004), may represent an immediate biophysical response, which may allow for a rapid adaptation to the water content and ion concentration or charge distribution in a given membrane compartment also *in vivo*.

5. Cubic Membranes: Indicators of Cellular Stress and Disease?

Notably, cubic membrane morphologies are often associated with deregulated protein synthesis, cellular stress, or more severe pathological conditions. This view, however, is perhaps somewhat biased since morphological abnormalities are typically investigated for diseased cells rather than for "wild type" conditions. Nevertheless, the correlation of specific membrane alterations in the course of acute or chronic cellular stresses needs closer consideration.

5.1. Virus-infected cells

Virus-induced membrane transitions, generally referred to as cytomembraneous inclusions, are a hallmark in experimental and pathological samples (Almsherqi *et al.*, 2005). However, due to the absence of a clear view of the 3D nature of these membrane structures, they appear under numerous nicknames in the literature, such as "tubulocrystalline inclusions" in HCV infected liver (Schaff *et al.*, 1992), "convoluted membraneous mass" in viral St. Louis Encephalitis (Murphy *et al.*, 1968), and "TRS" in SIV (Kaup *et al.*, 2005) and SARS-virus infected Vero cells (Goldsmith *et al.*, 2004).

The unexplained mechanism behind the formation of convoluted cubic membranes upon viral infection starts to unfold based on the structural similarity to crystalloid ER membranes induced by overexpression of HMG-CoA reductase in UT-1, or the parental CHO cells (Fig. 6.5), as well as in A-431 (human epidermal carcinoma) cells. Some evidence suggests that virus infection and deregulation of HMG-CoA reductase are mechanistically linked, resulting in similar membrane phenotypes. For example, West Nile Virus infection is associated with local cholesterol alterations of the plasma membrane of the host cell that leads to a sequestration of membraneous sites of viral replication (Mackenzie *et al.*, 2007). Depletion

of cholesterol in the plasma membrane triggers HMG-CoA reductase upregulation and consequently leads to the formation of a crystalloid (cubic or hexagonal) ER membrane. The virus-induced convoluted membrane was reported to be essential for viral replication and survival: administration of cholesterol that reverses the HMG-CoA reducase-induced convoluted membrane formation in the infected cells significantly suppresses viral replication (Mackenzie *et al.*, 2007). A recent study has also shown that virus-induced membrane complexes might provide partial protection against the host immune response (Hoenen *et al.*, 2007) and hence offer a site for efficient viral replication (Mackenzie *et al.*, 2007) or facilitate nucleo-cytoplasmic transport of genetic material (Almsherqi *et al.*, 2008).

5.2. Neoplasia

Cubic membranes (often labeled as TRS) have been reported to occur in the cytoplasm of breast carcinoma (Seman *et al.*, 1971), subcutaneous myxoma (Stoebner *et al.*, 1972), malignant lymphoma (Uzman *et al.*, 1971), in the nucleus of human osteosarcoma cells (Murray *et al.*, 1983), alveolar cell carcinoma (Ghadially *et al.*, 1985), and gastric adenocarcinoma (Caruso, 1991). Since viral infections frequently lead to cubic membrane formation, it would not be surprising to observe cubic membrane structures also in cases of virus-related tumors, such as leukemias, lymphomas, and in virus-induced hepatocellular carcinoma (Uzman *et al.*, 1971). TRS appear to be nonspecific to tumor differentiation or malignancy as they develop in highly replicative undifferentiated cells as well as in differentiated tumor cells. Therefore, due to the limited number of reported cases of cubic membrane structure in neoplastic cells, they currently are not yet diagnostically useful in the classification of tumors or in clinical prognosis. However, TRS could be used as a marker for viral-induced neoplasia, for example, hairy cell leukemia (Mantovani *et al.*, 1986).

5.3. Muscular dystrophy

Several muscular and neuromuscular diseases are associated with periodic membrane transformation of t-tubules of striated muscles, usually referred to as honeycomb structures. T-tubular morphological membrane transformation has been described in denervated muscles (Gori, 1972; Madarame *et al.*, 1986; Miledi and Slater, 1969; Pellegrino and Franzini, 1963), in the muscles with induced experimental myopathy (Macdonald and Engel, 1970), bupivacaine-induced myonecrosis (Huxley and Taylor, 1958), and in tenotomized muscles of the rat (Andreev and Wassilev, 1994). They have also been observed in various human muscles as a consequence of muscular diseases (Borg *et al.*, 1989; Cornog and Gonatas, 1967; Engel and Dale, 1968; Engel and Macdonald, 1970; Gori, 1972; Iorio Di *et al.*, 1989;

Miike *et al.*, 1984). The fact that cubic membrane organization appears under pathological conditions of myopathy support the notion that they may be formed in response to stress conditions, such as a decrease in cell volume in the case of muscular dystrophy. Thus, it could be speculated that the potential function of cubic membrane structures is to maintain cellular integrity by regulating the volume of the cell (organelle) and/or to accommodate stress-induced membrane-resident proteins. Interestingly, induced formation of honeycomb t-tubules may also be part of a developmental program as these membrane structures are also observed in tadpole tail muscles that spontaneously degenerate during metamorphosis (Sasaki *et al.*, 1985). Frequent transformation of t-tubules into G-type cubic membrane (honeycomb) organization in regenerating muscle fibers post pathological or experimentally induced muscular dystrophy may reflect the adaptive reorganization of the membrane system in the regenerating cell.

5.4. Autoimmune disease

Cubic membranes (including those labeled as TRS) have been frequently reported to occur under conditions and in cell types with an immunological background, for instance in diseases in which autoantibody production is a main factor in the pathogenesis. These include diffuse connective tissue diseases such as systemic and discoid lupus erythematosus (Grimley and Schaff, 1976) and Sjögren syndrome (Nakamura, 1974) or organ limited diseases, such as thyroiditis, gastritis, myasthenia gravis, and celiac disease (Helder and Feltkamp-Vroom, 1974). TRS are also reported in autoimmune diseases characterized by deposition of immune complexes or factors, which are discrete in comparison to the diffuse connective tissue diseases like rheumatoid arthritis, nephritis, and amyloidosis (Helder and Feltkamp-Vroom, 1974). Indeed, cubic membrane organization is frequently reported in immune deficiency diseases such as HIV (Kaup *et al.*, 2005). Such ultrastructural membrane alterations are often reported in endothelial cells and in lymphocytes; therefore, TRS should be regarded as potential markers of autoimmune diseases that are of a systemic nature.

6. Cubic Membranes: Specific Functions or Innocent Bystanders?

The frequent appearance of cubic membranes in several specialized cell types, in response to environmental conditions, stress or infection, poses the intriguing question as to their specific functions. It is possible that cubic membranes are but an inevitable self-assembled product of the complex molecular mixture of lipids and proteins, the result of ''simple'' molecular packing considerations and inter-molecular interactions. Even though this is

appealing to the long and unresolved debate about ''nonlamellar'' lipids in conjunction with cell membranes, an increasing body of evidence suggests that these structural organizations might have to fulfill a purpose and their formation cannot be rationalized solely by spontaneous molecular packing. It is important to stress that the proposed functions of cubic membranes in the following discussion are hypothetical, although recent experimental data provide support to some of these hypotheses.

6.1. Cell space organization and subvolume regulation

Continuous hyperbolic layers, as represented by cubic membranes, partition space into discrete and unconnected subvolumes. By definition, a multimembraneous structure consisting of (n) membranes, partitions space into ($n + 1$) physically distinct, intertwined, but separate subspaces. The identity of each space itself is not a consequence of the existence of a cubic membrane; rather it is an effect of a topologically invariant membrane morphogenesis. Although an intracellular space maintains its identity as long as membrane continuity is preserved, it is only by means of a hyperbolic membrane structure that such spatial relations can be rigorously defined. The identification of cubic membranes in multiple cell types and tissues clearly demonstrates that continuous intracellular membranes are much more frequently adopted than generally acknowledged.

6.2. Inter- and intracellular trafficking

Intracellular and inter-organelle trafficking of macromolecules and communication are active areas of research, yet no unified model exists. To what extent intracellular trafficking depends on or can be optimized through specific types of membrane organization, for example, as continuous 3D space partitioners or networks, is unknown. In the three dimensions of a cell, the partitioning of the intracellular space into subvolumes—leading to an interpenetrated pipeline system—could in principle be orchestrated by membrane organization, which ultimately controls spatio-temporal activities, including intracellular trafficking and transportation, and fast response to physiological alterations such as changing temperature, osmolarity or pH. Recognition of the existence of topologically distinct spaces through the formation of cubic membranes implies that cell space is restricted and predetermined to maintain distinct but interconnected subcellular domains. Cubic membranes may induce enrichment—or exclusion—of certain lipids and proteins, as a prerequisite for vesicle-mediated subcellular trafficking. They may also function as partitioners within a membrane, to create subdomains of specific molecular composition and function. It has been repeatedly noted that the stage of cell division and differentiation has a strong influence on the formation of cubic membranes. Cells that undergo rapid cell division and

differentiation, such as the differentiating sieve elements, cells during spermatogenesis, or tumor cells are well over-represented in the collection of cubic-membrane forming cells (Table 6.1). Obviously, during cell division and differentiation events, there is a greater need for regulated spatio-temporal transport, as well as cellular communication, which is particularly well illustrated during spermatogenesis (Table 6.1). In the case of differentiating sieve elements, cubic membranes might have a particular role in the assimilated transport process. Finally, it is of interest to note that aggregates of "synaptic vesicles" often resemble cubic membranes. This can be taken as an indication of a possible on-off mechanism of membrane continuity, which might account for a regulative capacity for the controlled release of transmitter substances.

6.3. Specific structure-function relationships

Several more general functionalities are under consideration for cubic membranes. In particular, a cubic bilayer arrangement could serve as a regulator of chemical or physical potentials across the membrane surface. This is indicated in several cases in which cubic membranes have been found to be sensitive to the growth medium. An osmo-regulative capacity of a plasma membrane-associated cubic membrane can be envisioned, which might serve to allow rapid adjustment to osmotic changes. Such a function is, for instance, consistent with the presence of cubic membranes in a variety of epithelial cells (Table 6.1). Cubic membranes may also be involved in curvature-controlled activation and regulation of membrane enzyme activities. For instance, diacylglycerols, which may function as second messengers to activate protein kinase C (PKC), display a strong propensity to form negatively curved membrane structures. The activity of PKC, however, is not specifically dependent on lipids that induce reverse hexagonal phases (Senisterra and Epand, 1993), and thus, reversed cubic phases. In view of the ubiquitous occurrence of cubic membranes it would be of interest to investigate the influence of PKC on cubic phases, and vice versa, to eventually correlate the geometry of the environment to protein activity.

Certain cubic membrane structures are apparently strongly linked to specific functions, such as the cubic structure found in the PLB of photosynthetic cells in higher plants. A physical role has been proposed for the selection of D-surface geometry (Guo *et al.*, 1995), based on theoretical considerations on how the geometry of crystals controls the emission or absorption of certain wavelengths of light through the existence of photonic band-gaps (Babin *et al.*, 2002). Although the D-surface is isotropic, its geometry is such that it may potentially trap photons. The absorbed energy could then be used by certain molecules that are positioned along a particular lattice direction, and, for instance, trigger conformational changes to revert PLB into an active thylakoid membrane geometry. A similar structural role can be considered for the selection of different subtypes of cubic

membrane architecture (photosome) in bioluminescent scaleworms (Bassot, 1964, 1966). Interestingly, the photosome membrane organization has a D subtype cubic membrane in the resting (unstimulated) state, however, upon electrical or optical stimulation the membrane configuration changes and acquires P subtype. Do different cubic membrane subtypes manipulate different wavelengths? Does the function of the cubic membrane change with the specific alteration of its geometrical configuration? The answers to these questions clearly deserve further investigations. In addition, several other photoactive cell types exist that contain cubic membranes. Mitochondria in the retinal cone of the tree shrew (*Tupaia glis*) (Foelix *et al.*, 1987) may adopt an isotropic membrane structure that allows efficient capture of the incoming light; in an alternative model, this multilayer G-surface cubic arrangement of the mitochondrial membrane (Fig. 6.7) may preferentially reflect UV light before reaching the outer segment of the retina, thus representing a specialized optical filter system.

7. Applications of Cubic Membranes

Although the specific functions of cubic membranes in biological systems are still to be uncovered, recent studies on the physical properties of such highly ordered membrane structures have suggested a range of potential applications, beyond conventional liposome technologies. Dispersed liquid crystalline phases such as bicontinuous cubic dispersions (known as Cubosomes®) have been the focus of recent studies as potential drug delivery agents (Barauskas *et al.*, 2005). Lipids forming cubic phases *in vitro* are also well-established matrices, for example, for membrane protein crystallization (Seddon *et al.*, 2004), but are not considered here in the context of cubic membranes.

7.1. DNA transfection

Cubic membrane function is potentially linked to intracellular trafficking processes for macromolecules. Indeed, isolated mitochondria with cubic membrane organization from starved amoeba cells (see above) have recently been shown to incorporate and retain short oligonucleotides (ODN) with high efficiency (Fig. 6.11) (Almsherqi *et al.*, 2008). Although the molecular basis for the high affinity of ODN to cubic membranes has not been uncovered yet, it is reasonable to assume that it is strongly promoted by electrostatic interactions with the highly curved and extended membrane surface. Furthermore, delivery of ODN-cubic membrane complexes to mammalian cells in culture appears to be very effective and might, therefore, provide an attractive alternative to currently employed cationic

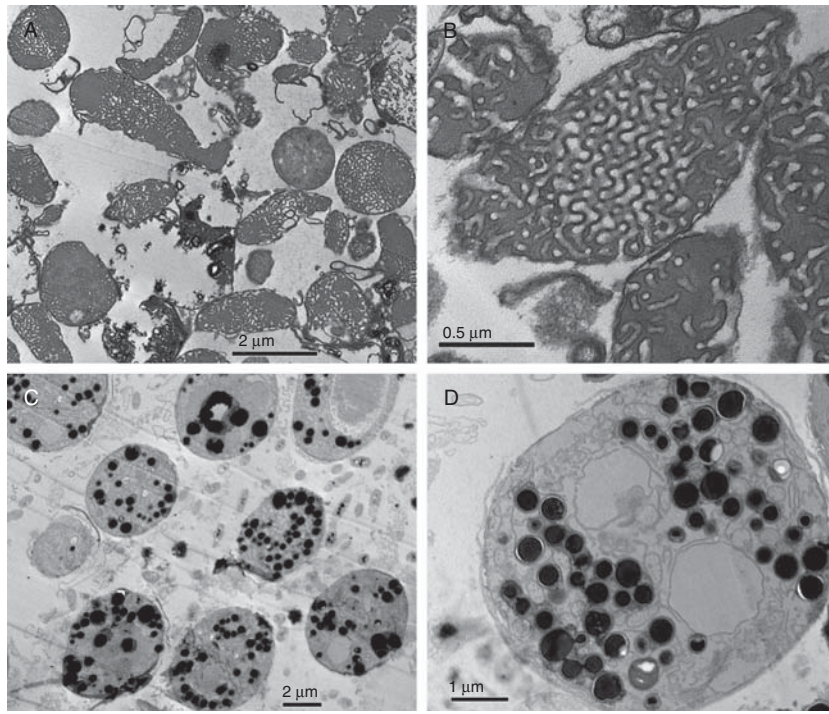

Figure 6.11 Cubic membrane organization and DNA uptake (Almsherqi *et al.*, 2008). (A) Low and (B) high magnification TEM images of mitochondria containing cubic membrane structure isolated from 10 d starved *Chaos* cells before (A and B) and after (C and D) incubation with ODNs. Multiple electron-dense intra-mitochondrial inclusions (D) may represent cubic membrane-mediated ODN interactions. The multiple pores (B) at the surface of mitochondria with cubic membrane organization may play an important role in facilitating passive uptake of ODNs.

lipoplexes and promises high efficacy and reduced cytotoxicity. Use of cubic membranes of biological origin as a carrier for DNA transfection or delivery of other nucleic acids, such as small interfering RNA and/or short hairpin RNA is currently under active investigation (Almsherqi *et al.*, 2008).

7.2. Do cubic membranes have optical properties?

The photonic properties of bi- or multicontinuous cubic phases based on triply periodic level surfaces (G, D, and P) have been extensively studied in materials science (Babin *et al.*, 2002; Maldovan *et al.*, 2002; Urbas *et al.*, 2002). In general, the lattice size of the photonic crystal has to be of the same magnitude as the wavelength range it controls. Photonic crystals based on triply periodic surfaces with the largest photonic band gaps known are of type D and G cubic morphology (Babin *et al.*, 2002). Similar G-surfaces describe

the cubic membrane organization of the inner mitochondrial membranes (Fig. 6.7) in the tree shrew's (*Tupaia belangeri*) retina (Foelix *et al.*, 1987) and photosynthesis-related membranes in prolamellar bodies of higher plants and chloroplasts of the green algae *Zygnema* (Fig. 6.6) (Deng, 1998; Deng and Landh, 1995). Based on these similar cubic geometries and relevant lattice sizes, it is tempting to speculate that perhaps *Tupaia* mitochondrial membranes and cubic membranes in *Zygnema* chloroplasts and PLB of higher plants may function as photonic crystals. The 12-layered cubic membrane organization of the mitochondria in retinal cones of tree shrew *Tupaia* and multilayer grana of photosynthetic membranes may thus enable these membranes to amplify, refract, or absorb certain wavelengths of light. Whether such an elaborate membrane arrangement is a protective response or whether it provides a specialized reaction center for embedded proteins awaits detailed analysis.

8. Concluding Remarks

The frequent appearance of nonlamellar membrane arrangements such as cubic membranes in cells under stressed or pathological conditions points to an intrinsic cellular response mechanisms. The extensive generation of membrane surfaces to facilitate exchange reactions between two (or more) sub-volumes, or the sequestration of specific lipids or proteins into membrane domains of nonlamellar morphology may provide a physiological advantage to cope with various stress phenomena. Current analyses of nonlamellar membrane arrangements are largely restricted to the descriptive level; the identification of inducible membrane systems, such as in virus-infected cells or the reversible transition of mitochondrial inner membranes of amoeba *Chaos* to cubic morphology upon starvation, however, opens new avenues for understanding the molecular mechanisms and cellular requirements underlying these membrane arrangements. Lipidomics and proteomics techniques on the one hand, and cryo-electron tomography on the other, hold great promise to uncover the mysteries of cubic membranes in living cells, in healthy and diseased states.

ACKNOWLEDGMENTS

The authors apologize to the colleagues whose work has not been cited due to space limitations. We thank Felix Margadant for critical reading of the manuscript, Mark Mieczkowski for the "Cubic Membrane Simulation Projection" program (QMSP), and Aik Kia Khaw for his art work presented in Fig. 6.4. The technical support by Chwee Wah Low, Li Ling Olivia Tan, and Mei Yin Shoon is gratefully acknowledged. Research in the authors' laboratories is supported by research grants NMRC (R-185-000-058-213) and BMRC from Singapore (R-185-000-065-305) to Y. D. and SFB Lipotox (project F3005) of the Austrian Science Fund to S.D.K.

REFERENCES

Adriaensen, D., Scheuemann, D. W., Timmermans, J.-P., and de Groodt-Lasseel, M. H. A. (1990). Neuroepithelial endocrine cells in the lung of the lungfish *Protopterus aetiopicus*. An electron and fluorescence-microscopical investigation. *Acta Anat.* **139,** 70–77.

Ahn, J. N. (1971). Myeloid bodies of the retinal pigment epithelium. I. Distribution, morphology and connections with cytoplasmic organelles. *Z. Zellforsch.* **115,** 508–523.

Allen, R. D. (2000). The contractile vacuole and its membrane dynamics. *Bioessays* **22,** 1035–1042.

Allen, R. D., and Fok, A. K. (1988). Membrane dynamics of the contractile vacuole complex of *Paramecium*. *J. Protozool.* **35,** 63–71.

Allen, R. D., Ueno, M. S., Pollard, L. W., and Fok, A. K. (1990). Monoclonal antibody study of the decorated spongiome of contractile vacuole complexes of *Paramecium*. *J. Cell Sci.* **96,** 469–475.

Almsherqi, Z. A., McLachlan, C. S., Mossop, P., Knoops, K., and Deng, Y. (2005). Direct template matching reveals a host subcellular membrane gyroid cubic structure that is associated with SARS virus. *Redox Rep.* **10,** 167–171.

Almsherqi, Z. A., Kohlwein, S. D., and Deng, Y. (2006). Cubic membranes: A legend beyond the Flatland* of cell membrane organization. *J. Cell Biol.* **173,** 839–844.

Almsherqi, Z., Hyde, S., Ramachandran, M., and Deng, Y. (2008). Cubic membranes: A structure-based design for DNA uptake. *J. R. Soc. Interface* **5,** 1023–1029.

Anderson, R. G., Orci, L., Brown, M. S., Garcia-Segura, L. M., and Goldstein, J. L. (1983). Ultrastructural analysis of crystalloid endoplasmic reticulum in UT-1 cells and its disappearance in response to cholesterol. *J. Cell Sci.* **63,** 1–20.

Anderson, R. H., and Zachariah, K. (1972). The effects of fixatives on lattice bodies and bundles in apothecial cells of the fungus Ascobolus. *Can. J. Bot.* **50,** 343–347.

André, J. J. (1959). Etude au microscope électronique de l'évolution du chondriome pendant la spermatogénèse du scorpion *Euscorpius flavicaudis*. *Ultrastruct. Res.* **2,** 288–308.

Andreev, D., and Wassilev, W. (1994). Tubular networks in soleus muscle fibers of the rat following tenotomy. I. Spatial organization. *Ann. Anat.* **176,** 87–91.

Arechaga, I., Miroux, B., Karrasch, S., Huijbregts, R., de Kruijff, B., Runswick, M. J., and Walker, J. E. (2000). Characterisation of new intracellular membranes in *Escherichia coli* accompanying large scale over-production of the b subunit of F(1)F(o) ATP synthase. *FEBS Lett.* **482,** 215–219.

Arsenault, A. L., Clattenburg, R. E., and Odense, P. H. (1979). Spermiogenesis in the shrimp, *Crangon septemspinosa,* Say. *Can. J. Zool.* **57,** 486–498.

Arsenault, A. L., Clattenburg, R. E., and Odense, P. H. (1980). Further observations on spermiogen esis in the shrimp, *Crangon septemspinosa*. A mechanism for cytoplasmic reduction. *Can. J. Zool.* **58,** 497–506.

Atoji, Y., Suzuki, Y., and Sugimura, M. (1989). The preputial gland of the Japanese serow: *Capricornus crispus*: Ultrastructure and lectin histochemistry. *Acta Anat. (Basel)* **134,** 245–252.

Awad, T. S., Okamoto, Y., Masum, S. M., and Yamazaki, M. (2005). Formation of cubic phases from large unilamellar vesicles of dioleoylphosphatidyl-glycerol/monoolein membranes induced by low concentrations of Ca^{2+}. *Langmuir* **21,** 11556–11561.

Babai, F., Tremblay, G., and Dumont, A. (1969). Intranuclear and intranucleolar tubular structures in Novikoff hepatoma cells. *J. Ultrastruct. Res.* **28,** 125–130.

Babin, V., Garstecki, P., and Holyst, R. (2002). Photonic properties of multicontinuous cubic phases. *Phys. Rev. B* **66,** 235120.1–235120.9.

Barauskas, J., Johnsson, M., Joabsson, F., and Tiberg, F. (2005). Cubic phase nanoparticles (Cubosome): Principles for controlling size, structure, and stability. *Langmuir* **21,** 2569–2577.

Barber, V. C. (1967). The sense organs of Nautilus: Preliminary observation on their fine structure. *J. Microsc. (France)* **6,** 1067–1072.
Barber, V. C., and Wright, D. E. (1969). The fine structure of the sense organs of the cephalopod mollusc. *Nautilus. Z. Zellforsch.* **102,** 293–312.
Baringer, J. R., and Griffith, J. F. (1970). Experimental herpes simplex encephalitis: Early neuropathologic changes. *J. Neuropathol. Exp. Neurol.* **29,** 89–104.
Barton, R. (1965). An unusual organelle in the peripheral cytoplasm of *Chara* cells. *Nature* **205,** 201.
Bassot, J.-M. (1964). Presence of a paracrystalline form of the endoplasmic reticulum in the photocytes of annelides Polyninæ. *C. R. Acad. Sci. Paris* **259,** 1549–1552.
Bassot, J.-M. (1966). A microtubular paracrystalline form of the endoplasmic reticulum in the photocyres of the Annelides polyninæ. *J. Cell Biol.* **31,** 135–158.
Bassot, J.-M., and Nicolas, M.-T. (1978). Similar paracrystals of endoplasmic reticulum in the photoemitters and the photoreceptors of scale-worms. *Experientia (Basel)* **34,** 726–728.
Bassot, J.-M., and Nicolas, M.-T. (1987). An optional dyadic junctional complex revealed by fast freeze fixation in the bioluminescent system of the scale worm. *J. Cell Biol.* **105,** 2235–2256.
Bassot, J.-M., and Nicolas, M.-T. (1995). Bioluminescence in scale worm photosomes: The photoprotein polynoidin is specific for the detection of superoxide radicals. *Histochem. Cell Biol.* **104,** 199–210.
Bauer, M., and Pelkmans, L. (2006). A new paradigm for membrane-organizing and -shaping scaffolds. *FEBS Lett.* **580,** 5559–5564.
Bawa, S. R., and Werner, G. (1988). Cyst and flagellar sheath formation in *Diplomentus* sp. spermiogenesi. *J. Ultrastruct. Mol. Struct. Res.* **101,** 51–61.
Beams, H. W., and Kessel, R. G. (1963). Electron microscope studies on developing crayfish oocytes with special reference to the origin of yolk. *J. Cell Biol.* **18,** 621–649.
Beams, H. W., and Kessel, R. G. (1977). Physical properties of blue-green algae: Ultracentrifugation and electron microscope studies. *Protoplasma* **92,** 229–242.
Behnke, H.-D. (1965). On the fine structure of a "lattice-like" body in the sieve elements of *Discorea reticulata*. *Planta* **66,** 106–112.
Behnke, H.-D. (1968). On the formation of lattice-like membrane structures in the sieve elements of *Dioscorea*. *Protoplasma* **66,** 287–310.
Behnke, H.-D. (1973). On relations between structural changes in the endoplasmic reticulum and the appearance of protein filaments in differentiating sieve tubes of *Smilax exceisa*. *Protoplasma* **77,** 279–289.
Behnke, H.-D. (1981). Sieve-element characters. *Nord. J. Bot.* **1,** 381–400.
Bell, M. (1974a). A comparative study of the ultrastructure of the sebaceous glands of man and other primates. *J. Invest. Dermatol.* **62,** 132–143.
Bell, M. (1974b). Effect of andogen on the ultrastructure of the sebaceous gland in two species. *J. Invest. Dermatol.* **62,** 202–210.
Bergeron, M., and Thiéry, G. (1981). Three-dimensional characteristics of the endoplasmic reticulum of rat renal tubule cell, an electron microscopy study in thick sections. *Biol. Cell* **42,** 43–48.
Berkaloff, C. (1967). Ultrastructural changes of the chloroplast thylakoids during the development of the encystment. *J. Microsc. (France)* **6,** 839–852.
Bertmar, G. (1972). Labyrinth cells, a new cell type in vertebrate olfactory organs. *Z. Zellforsch.* **132,** 245–256.
Bilbaut, A. (1980). Cell junctions in the excitable apithelium of bioluminescent scales on a polynoid worm: A freeze-fracture and electrophysiological study. *J. Cell. Sci.* **41,** 341–368.

Black, V. (1972). The development of smooth-surfaced endoplasnime reticulum in adrenal cortical cells of fetal guinea pigs. *Am. J. Anat.* **135,** 381–417.

Blanchette, E. J. (1966a). Ovarian steroid cells. I. Differentiation of the lutein cell from the granulosa follicle cell during the preovulatory stage and under the influence of exogenous gonadotropin. *J. Cell Biol.* **31,** 501–516.

Blanchette, E. J. (1966b). Ovarian steroid cells. II. The lutein cell. *J. Cell. Biol.* **31,** 517–542.

Blinzinger, K., Simon, J., Magrath, D., and Boulger, L. (1969). Poliovirus crystals within the endoplasmic reticulum of endothelial and mononuclear cells in the monkey spinal cord. *Science* **163,** 1336–1337.

Blinzinger, K., Anzil, A. P., and Deutschlander, N. (1972). Nature of tubular aggregates. *N. Engl. J. Med.* **286,** 157–158.

Bocquet, M., and Dhainaut-Courtois, N. (1973). Fine structure of the photoreceptor organ of the *Syllidae* (Annélides polychètes). *J. Microsc. (France)* **18,** 207–230.

Bolender, R. P., and Weibel, E. R. (1973). A morphometric study of the removal of phenobarbital induced membranes from hepatocytes after cessation of treatment. *J. Cell Biol.* **56,** 746–761.

Borg, K., Solders, G., Borg, J., Edström, L., and Kristensson, K. (1989). Neurogenic involvement in distal myopathy (Welander). Histochemical and morphological observations on muscle and nerve biopsies. *J. Neurol. Sci.* **91,** 53–70.

Borysko, E., and Roslansky, J. (1959). Methods for correlated optical and electron microscopic studies of amoebae. *Ann. N. Y. Acad. Sci.* **78,** 432–447.

Bouligand, Y. (1990). Comparative geometry of cytomembranes and water-lipid systems. *J. Phys. (France)* **51,** C735–C752.

Bouligand, Y. (1991). Geometry and topology of cell membranes. In: "Geometry in Condensed Matter Physics" (J. F. Sadoc, Ed.) pp. 193-231, Word Scientific Press, London.

Bourgeois, C. A., and Hubert, J. (1988). Spatial relationship between the nucleolus and the nuclear envelope: Structural aspects and functional significance. *Int. Rev. Cytol.* **111,** 1–52.

Brammer, J. D., and White, R. H. (1969). Vitamin A deficiency: Effect on mosquito eye ultrastructure. *Science* **163,** 821–823.

Brandenburg, K., Koch, M. H., and Seydel, U. (1990). Phase diagram of lipid A from *Salmonella minnesota* and *Escherichia coli* rough mutant lipopolysaccharide. *J. Struct. Biol.* **105,** 11–21.

Brandenburg, K., Koch, M. H., and Seydel, U. (1992). Phase diagram of deep rough mutant lipopolysaccharide from *Salmonella minnesota* R595. *J. Struct. Biol.* **108,** 93–106.

Brandt, P. W., and Pappas, G. D. (1959). Mitochondria. II. The nuclear-mitochondrial relationship in Pelomyxa carolinensis Wilson (*Chaos chaos L.*). *J. Biophys. Biochem. Cytol.* **6,** 91–95.

Brites, P., Waterham, H. R., and Wanders, R. J. (2004). Functions and biosynthesis of plasmalogens in health and disease. *Biochim. Biophys. Acta* **1636,** 219–231.

Bryan, G. W., Zadylak, H. A., and Ehret, C. F. (1967). Photoinduction of plastid and of chlorophyll in a *Chlorella* mutant. *J. Cell Sci.* **2,** 513–528.

Cameron, C. H., Kenny, B. D., Clements, W. D. B., and Toner, P. G. (1992). Unusual extraskeletal myxoid chodrosarcoma. *Ultrastruct. Pathol.* **16,** 17–23.

Canese, M. G., Rizzeto, M., Novara, R., London, W. T., and Purcell, R. H. (1984). Experimental infection of chimpanzees with the HBsAg-associated delta (δdL) agent: An ultrastructural study. *J. Med. Virol.* **13,** 63–72.

Cannon, M. S., and Hostetler, J. R. (1976). The anatomy of the parotoid gland in *Bufonidae* with some histochemical findings. II. *Bufo alvarius*. *J. Morphol.* **148,** 137–160.

Caruso, R. A. (1991). Intranuclear and intranucleolar tubular inclusions in gastric adenocarcinoma cells. *Ultrastruct. Pathol.* **15,** 139–148.

Casey, H. W., Woodruff, J. M., and Butcher, W. I. (1967). Electron microscopy of a benign epidermal pox disease of rhesus monkeys. *Am. J. Pathol.* **51,** 431–446.
Cavicchia, J. C., and Moviglia, G. A. (1982). Fine structure of the testis in the toad (*Bufo arenarum Hensel*): A freeze-fracture study. *Anat. Rec.* **203,** 463–474.
Chaigneau, J. Z. (1971). The organ of Bellonci of the crustacea isopoda *Sphaeroma serratum* (Fabricius). Ultrastructure and meaning. *Z. Zellforsch.* **112,** 166–187.
Chandra, S. (1968). Undulating tubules associated with endoplasmic reticulum in pathological tissue. *Lab. Invest.* **18,** 422–428.
Chandra, S., and Stefani, S. S. (1976). A possible mode of formation of tubuloreticular structures. *J. Ultrastruct. Res.* **56,** 304–311.
Chen, I.-L., and Yates, R. D. (1967). An ultrastructural study of opaque cytoplasmic inclusions induced by triparanol treatment. *Am. J. Anat.* **121,** 705–726.
Cheville, N. F. (1966). The cytopathology of swine pox in the skin of swine. *Am. J. Pathol.* **49,** 339–352.
Chin, D. J., Luskey, K. L., Anderson, R. G., Faust, J. R., Goldstein, J. L., and Brown, M. S. (1982). Appearance of crystalloid endoplasmic reticulum in compactin-resistant Chinese hamster cells with a 500-fold increase in 3-hydroxy-3-methylglutaryl-coenzyme A reductase. *Proc. Natl. Acad. Sci. USA* **79,** 1185–1189.
Chiradella, H. (1989). Structure and development of iridescent butterfly scales: Lattice and laminae. *J. Morphol.* **202,** 69–88.
Chiradella, H. (1994). Structure of butterfly scales: Patterning in an insect cuticle. *Microsc. Res. Tech.* **27,** 429–438.
Christensen, A. K., and Fawcett, D. W. (1966). The fine structure of testicular interstitial cells in mice. *Am. J. Anat.* **118,** 551–572.
Clark, A. W. (1967). Some aspects of spermiogenesis in a lizard. *Am. J. Anat.* **121,** 369–400.
Coakley, W. T., and Gallez, D. (1989). Membrane-membrane contact: Involvement of interfacial instability in the generation of discrete contacts. *Biosci. Rep.* **9,** 675–691.
Cornog, J. L., and Gonatas, N. K. (1967). Ultrastructure of rhabdomyoma. *J. Ultrastruct. Res.* **20,** 433–450.
Cotelli, F., and Donin, L. L. C. (1980). The spermatozoan of *Peracarida*. II. The spermatozoan of *Tanaidacea*. *J. Ultrastruct. Res.* **73,** 263–268.
Crawley, J. C. W. (1965). A cytoplasmic organell associated with the cells walls of *Chara* and *Nitella*. *Nature* **205,** 200–201.
Daniels, E. W., and Breyer, E. P. (1965). Differences in mitochondrial fine structure during mitosis in amoebae. *J. Protozool.* **12,** 417–422.
Daniels, E. W., and Breyer, E. P. (1967). Ultrasructure of giant amoeba *Pelomyxa palustris*. *J. Protozool.* **14,** 167–179.
Daniels, E. W., and Breyer, E. P. (1968). Starvation effects on the ultrastructure of amoeba mitochondria. *Z. Zellforsch.* **91,** 159–169.
Daniel, J. W., and Järlfors, U. (1972a). Plasmodial ultrastructure of the myxomycete *Physarum polycephalim*. *Tissue Cell* **4,** 15–36.
Daniel, J. W., and Järlfors, U. (1972b). Light-induced changes in the ultrastructure of a plasmodial myxomycete. *Tissue Cell* **4,** 405–426.
de Campo, L., Yaghmur, A., Sagalowicz, L., Leser, M. E., Watzke, H., and Glatter, O. (2004). Reversible phase transitions in emulsified nanostructured lipid systems. *Langmuir* **20,** 5254–5261.
de Ceccatty, P. M., Bassot, J. M., Bilbaut, A., and Nicolas, M.-T. (1977). Bioluminescence of the elytras of Acholoe. I. Morphological support for its structure. *Biol. Cell* **28,** 57–64.
Delfino, G., Turillazzi, S., and Calloni, C. (1988). A light and electron microscope study on the Dufour's gland in *Parischnogaster* (Hymenoptera: Stenograstrinae). *Z. Mikrosk. Anat. Forsch.* **102,** 627–644.

Deng, Y. (1998). Transmission electron microscopy studies of cubic membrane morphologies in chloroplasts of the green algae *Zygnema* and mitochondria of the amoeba *Chaos carolinensis*. *In* PhD thesis p. 144. State University of New York at Buffalos, USA.

Deng, Y., and Landh, T. (1995). The cubic gyroid-based membrane structure of the chloroplast in Zygnema (*Chlorophyceae zygnematales*). *Zool. Stud.* **34,** 175–177.

Deng, Y., and Mieczkowski, M. (1998). Three-dimensional periodic cubic membrane structure in the mitochondria of amoebae *Chaos carolinensis*. *Protoplasma* **203,** 16–25.

Deng, Y., Marko, M., Buttle, K. F., Leith, A., Mieczkowski, M., and Mannella, C. A. (1999). Cubic membrane structure in amoeba (*Chaos carolinensis*) mitochondria determined by electron microscopic tomography. *J. Struct. Biol.* **127,** 231–239.

Deng, Y., Kohlwein, S. D., and Mannella, C. A. (2002). Fasting induces cyanide-resistant respiration and oxidative stress in the amoeba Chaos carolinensis: Implications for the cubic structural transition in mitochondrial membranes. *Protplasma* **219,** 160–167.

Dorsett, D. A., and Hyde, R. Z. (1968). The fine structure of the lens and photoreceptor of *Neries virens*. *Z. Zellforsch.* **85,** 243–255.

Dudkina, N. V., Heinemeyer, J., Keegstra, W., Boekema, E. J., and Braun, H. (2005). Structure of dimeric ATP synthase from mitochondria: An angular association of monomers induces the strong curvature of the inner membrane. *FEBS Lett.* **579,** 5769–5772.

Eakin, R. M., and Brandenburger, J. L. (1975). Retinal differences between light-tolerant and light avoiding slugs (*Mollusca: Pulmonata*). *J. Ultrastruct. Res.* **53,** 382–394.

Eakin, R. M., and Brandenburger, J. L. (1985). Effects of light and dark on photoreceptors in the polychaete annelid Nereis limnicola. *Cell Tissue Res.* **242,** 613–622.

Eckelbarger, K. J. (1982). Undulating arrays of endoplasmic reticulum in the spermatids of an opisthobranch mollusc. *J. Tissue Cell.* **14,** 289–295.

Eckelbarger, K. J., and Eyster, L. S. (1981). An ultrastructural study of spermatogenesis in the nudibranch mollusc *Spurilla neapolitana*. *J. Morphol.* **170,** 283–299.

Elliott, A. M., and Bak, I. L. (1964). The contractile vacuole and related structures in *Tetrahymena pyriformis*. *J. Protozool.* **11,** 250–261.

Engel, A. G., and Dale, A. J. D. (1968). Autophagic clycogenosis of late onset with mitochondrial abnormalities: Light and electron microscopic observations. *Mayo Clin. Proc.* **43,** 233–279.

Engel, A. G., and Macdonald, R. D. (1970). Ultrastructural reactions in muscle disease and their light-microscopic correlates. *In*: ''Muscle Diseases'' (J. N. Walton, N. Canal, and G. Scarlato, Eds.), pp. 71–89. Excerpta Medica, Amsterdam.

Esau, K., and Gill, R. H. (1971). Aggregation of endoplamic reticulum and its relation to the nucleus in a differentiating sieve element. *J. Ultrastruct. Res.* **34,** 144–158.

Esau, K., and Hoefert, L. (1980). Endoplasmic reticulum and microtubules in sieve elements. *J. Ultrastruct. Res.* **71,** 249–257.

España, C., Brayton, M. A., and Reubner, B. H. (1971). Electron microscopy of the Tana poxvirus. *Exp. Mol. Pathol.* **15,** 34–42.

Evert, R. F., and Deshpande, B. P. (1969). Electron microscope investigation of sieve-element ontogeny and structure in *Ulmus americana*. *Protoplasma* **68,** 403–432.

Eymé, J. (1963). Observation cytologiques sur les nectaries de trios renonculacées. *Le Botaniste* **46,** 137–179.

Eymé, J. (1967). Nouvelles observatinos sur l'infrastructure de tissus nectarigénes floraux. *Le Botaniste* **50,** 169–183.

Eymé, J., and Blance Le, M. (1963). Contribution à l'étude inframicroscopique d'inclusions cytoplasmiques présentes dans les ovules de *Ficaria* et dans les nectaries d'*Helloborus*. *C. R. Acad. Sci. (Paris)* **256,** 4958–4959.

Eymé, J. C. R. (1966). Infrastructure des cellules nectarigénes de *Diplotaxis erucoides* D. C., *Helleborus niger* L. et *H.fœtidus* L. *C. R. Acad. Sci. (Paris) Serie D.* **262,** 1629–1632.

Fahrenbach, W. H. (1964). The fine structure of naupilius eye. *Z. Zellforsch.* **62,** 182–197.

Fain-Maurel, M.-A., and Cassier, P. Z. (1969). Mitochondrial pleomorphism in the corpora allata of *Locusta migratoria migratorioides* in the course of imaginal life. *Z. Zellforsch.* **102,** 543–553.

Fain-Maurel, M.-A., and Cassier, P. J. (1972). On a new modality of the arrangement in "cotte de mailles" of the endoplasmic reticulum. *J. Microsc. (France)* **14,** 121–124.

Fain-Maurel, M.-A., and Cassier, P. J. (1973). Diversity of mitochondrial types in an absorbant cell and description of a new geometric arrangement of cristae. *J. Microsc. (France)* **16,** 279–286.

Foelix, R. F., Kretz, R., and Rager, G. (1987). Structure and postnatal development of photoreceptors and their synapses in the retina of the tree shrew (*Tupaia belangeri*). *Cell Tissue Res.* **247,** 287–297.

Fok, A. K., Aihara, M. S., Ishida, M., Nolta, K. V., Steck, T. L., and Allen, R. D. (1995). The pegs on the decorated tubules of the contractile vacuole complex of *Paramecium* are proton pumps. *J. Cell Sci.* **108,** 3163–3170.

Folliot, R., and Maillet, P. L. (1965). On a transitory functional aspect of the endoplasmic reticulum during spermatogenesis of *Dysderus fasciatus* Sign. (*Hemiptera pyrrhocoridaei*). *C. R. Soc. Biol.* **159,** 2483–2485.

Franceshi, V. R., and Lucas, W. J. (1980). Structure and possible function(s) of charasomes; complex plasmalemmae-cell wall elaborations present in some characean species. *Protoplasma* **104,** 253–271.

Franceshi, V. R., and Lucas, W. J. (1981). The charasome periplasmic space. *Protoplasma* **107,** 269–284.

Franke, W. W., and Scheer, U. (1971). Some structural differentiations in HeLa cell: Heavy bodies, annulate lamellae, and cotte de maillet endoplasmic reticulum. *Cytobiologie* **4,** 317–329.

Friedberg, I., Goldberg, I., and Ohad, I. (1971). A prolamellar body-like structure in *Chlamydomonas reinhardi*. *J. Cell Biol.* **50,** 268–275.

Fringes, B., and Gorgas, K. (1993). Crystalloid smooth endoplasmic reticulum in the Quail uropygial gland. *Ann. Anat.* **175,** 231–235.

Gales, T. L., Mazzulla, M. J., Kallender, H., Hill, F., and Maleeff, B. E. (2002). Ultrastructural characterization of ATP Synthase subunit b overexpression in *E. coli*. *Midrosc. Microanal.* **8**(Suppl 2), 984–985CD.

Garrosa, M., and Coca, S. (1991). Postnatal development of the vomeronasal epithelium in the rat: An ultrastructural study. *J. Morphol.* **208,** 257–269.

Geha, R. S., Schneeberger, E., Gatien, J., Rosen, F. S., and Merler, E. (1974). Synthesis of an M component by circulating B lymphocytes in severe combined immunodeficiency. *N. Engl. J. Med.* **290,** 726–728.

Ghadially, F. N. (1988). Ultrastructural Pathology of the Cell and Matrix Butterworths, London.

Ghadially, F. N., Harawi, S., and Khan, W. (1985). Diagnostic ultrastructural markers in alveolar cell carcinoma. *J. Submicrosc. Cytol.* **17,** 269–278.

Goldsmith, C. S., Tatti, K. M., Ksiazek, T. G., Rollin, P. E., Comer, J. A., Lee, W. W., Rota, P. A., Bankamp, B., Bellini, W. J., and Zaki, S. R. (2004). Ultrastructural characterization of SARS coronavirus. *Emerg. Infect. Dis.* **10,** 320–326.

Gonzales-Crussim, F., and Manz, H. J. (1972). Structure of a hepatomblastoma of pure epithelial type. *Cancer* **29,** 1272–1280.

Gori, Z. (1972). Proliferations of the sarcoplasmic reticulum and the T-system in denervated muscle fibers. *Virchows Arch. B. Zellpathol.* **11,** 147–160.

Granhall, U., and von Hofsten, A. (1969). The ultrastructure of a cyanophage attack *Anabaena variablis*. *Physiol. Plant.* **22,** 713–722.

Granick, S. (1961). The chloroplast: Inheritance, structure and function. *In*: "The Cell. Biochemistry, Physiology, Morphology" (J. Brachet and A. Mirsky, Eds.), Vol II, pp. 489–602. Academic Press, New York.

Grimley, P. M., and Schaff, Z. (1976). Significance of tubuloreticular inclusions in the pathobiology of human diseases. *Pathobiol. Annu.* **6,** 221–257.

Grimley, P. M., and Demsey, A. (1980). Functions and alterations of cell membranes during active virus infection. *In*: "Pathobiology of Cell Membranes" (B. F. Trump and A. U. Arstila, Eds.), Vol II, pp. 94–168. Academic Press, New York.

Guatelli, J. C., Porter, K. R., Anderson, K. L., and Boggs, D. P. (1982). Ultrastructure of the cytoplasmic and nuclear matrice of human lymphocytes observed using high voltage electron microscopy of embedment-free sections. *Biol. Cell* **43,** 69–80.

Gunning, B. E. S. (1965). The greening process in plastids. 1. The structure of the prolamellar body. *Protoplasma* **60,** 111–130.

Gunning, B. E. S., and Jagoe, M. P. (1967). The prolamellar body. *In*: "Biochemistry of Chloroplasts" (T. W. Goodwin, Ed.), Vol II, pp. 656–676. Academic Press, New York.

Gunning, B. E. S., and Steer, M. W. (1975). Ultrastructure and Biology of Plant Cells Arnold Publisher, London.

Guo, Y., Mieczkowski, M., and Landh, T. (1995). The prolamellar body as a cubic cytomembrane with double diamond symmetry: A putative photon blocker. *Biophys. J.* **68,** A240.

Gupta, B. L., and Smith, D. S. (1969). Fine structural organization of the spermatheca in the cockroach *Periplanta americana*. *Tissue Cell* **1,** 295–324.

Gutierrez, M., and Aoki, A. (1973). Fine structure of the gular gland of the free-tailed bat *Tadarida brasiliensis*. *J. Morphol.* **141,** 293–296.

Hashimoto, I. A., Hagiwara, A., and Komatsu, T. (1984). Ultrastructural studies on the pathogenesis of poliomyelitis in monkeys infected with poliovirus. *Acta Neuropathologica* **64,** 53–60.

Hatae, T. (1990). Membranous body in the jejunal absorptive cells of suckling rat intestine. *J. Electron Microsc.* **39,** 178–181.

Hausmann, K., and Allen, R. D. (1977). Membranes and microtubules of the excretory apparatus of *Paramecium caudatum*. *Cytobiologie* **15,** 303–320.

Helder, A. W., and Feltkamp-Vroom, T. M. (1974). Tubuloreticular structures and anti-nuclear antibodies in autoimmune and non-autoimmune diseases. Virus-like Structures in Human Tissues, (A. W. Helder, Ed.). University of AmesterdamAcademic thesis.

Hirosawa, K. (1992). Well-developed networks of smooth endoplasmic reticulum in Müller cell cytoplasma of the pika retina. *In*: "Electron Microscope H-7000, Hitachi, LTD., marketing catalog No. EX-E646" p. 6. Tokyo, Japan.

Hobman, T. C., Woodward, L., and Farquhar, M. G. (1992). The rubella virus E1 glycoprotein is arrested in a novel post-ER, pre-Golgi compartment. *J. Cell Biol.* **118,** 795–811.

Hoenen, A., Liu, W., Kochs, G., Khromykh, A. A., and Mackenzie, J. M. (2007). West Nile virus-induced cytoplasmic membrane structures provide partial protection against the interferon-induced antiviral MxA protein. *J. Gen. Virol.* **88,** 3013–3017.

Holtzman, E., Freeman, A. R., and Kashner, L. A. (1970). A cytochemical and electron microscope study of channels in the Schwann cells surrounding lobster giant axons. *J. Cell Biol.* **44,** 438–445.

Hoober, J. K., Siekevitz, P., and Palade, G. E. (1969). Formation of chloroplast membranes in Chlamydomonas reinhardi y-1. Effects of inhibitors of protein synthesis. *J. Biol. Chem.* **244,** 2621–2631.

Hooper, G. R., and Wiese, M. V. (1972). Cytoplasmic inclusions in wheat affected by wheat spindle streak mosaic. *Virology* **47,** 664–672.

Horvath, E., Kovacs, K., Szabo, S., Garg, B. D., and Tuchweber, B. (1973). Effect of cycloheximide on the fine structure of *corpus luteum* in intact and hypophysectomized rats. *Z. Zellforsch. Mikrosk. Anat.* **146,** 223-235.

Hostetler, J. R., Cannon, M. S., and Belt, W. D. (1976). Crystalloid configuration in the adrenal cortex of the Siamese tree shrew (*Tupaia glis*). *Anat. Rec.* **185,** 381–388.
Hourdry, J. (1969). Degenerative phenomena in the intestine epithelium of the tadpole of *Alytes obstetricans* Laur. *Z. Zellforsch.* **101,** 527–554.
Hruban, Z., Mochizuki, Y., Morris, H. P., and Slesers, A. (1972). Endoplasmic reticulum, lipid, and glycogen of Morris hepatosomas. Comparisons with alterations in hepatocytes. *Lab. Invest.* **26,** 86–99.
Hsieh, C. E., Leith, A., Mannella, C. A., Frank, J., and Marko, M. (2006). Towards high-resolution three-dimensional imaging of native mammalian tissue: Electron tomography of frozen-hydrated rat liver sections. *J. Struct. Biol.* **153,** 1–13.
Huxley, A. F., and Taylor, R. E. (1958). Local activation of striated muscle fibres. *J. Physiol.* **144,** 426–441.
Hyde, S., Andersson, S., Larsson, K., Blum, Z., Landh, T., Lidin, S., and Ninham, B. (1996). Cytomembranes and cubic membrane systems revisited. *In*: ''The Language of Shape''. pp. 257–338. Elsevier, Amsterdam.
Ikeda, T. (1968). Analytical studies on the structure of prolamellar body. *Bot. Mag. (Tokyo)* **81,** 517–527.
Iorio di, G., Lus, G., Cutillo, C., Cecio, A., and Cotrufo, R. (1989). Histopathological heterogeneity and cytopathological similarity of findings in different muscles of two brothers affected by rigid spine syndrome. *J. Neurol. Sci.* **94,** 107–114.
Ishida, M., Aihara, M. S., Allen, R. D., and Fok, A. K. (1993). Osmoregulation in *Paramecium*: The locus of fluid segregation in the contractile vacuole complex. *J. Cell Sci.* **106,** 693–702.
Ishida, M., Fok, A. K., Aihara, M. S., and Allen, R. D. (1996). Hyperosmotic stress leads to reversible dissociation of the proton pump-bearing tubules form the contractile vacuole complex in *Paramecium*. *J. Cell Sci.* **109,** 229–237.
Ishikawa, T. (1963). Fine structure of retinal vessels in man and the macaque monkey. *Invest. Ophtalmol.* **2,** 1–15.
Ishikawa, H. (1968). Formation of elaborate networks of T-system tubules in cultured skeletal muscle with special reference to the T-system formation. *J. Cell Biol.* **38,** 51–66.
Israelachvili, J. N., and Wolfe, J. (1980). The membrane geometry of the prolamellar body. *Protoplasma* **100,** 315–321.
Jenkinson, D. M., Elder, H. Y., Montgomery, I., and Moss, V. A. (1985). Comparative studies of the ultrastructure of the sebaceous gland. *Tissue Cell* **17,** 683–698.
Jingami, H., Brown, M. S., Goldstein, J. L., Anderson, R. G., and Luskey, K. L. (1987). Partial deletion of membrane-bound domain of 3-hydroxy-3-methylglutaryl coenzyme A reductase eliminates sterol-enhanced degradation and prevents formation of crystalloid endoplasmic reticulum. *J. Cell Biol.* **104,** 1693–1704.
John, G. B., Shang, Y., Li, L., Renken, C., Mannella, C. A., Selker, J. M. L., Rangall, L., Bennett, M. J., and Zha, J. (2005). The mitochondrial inner membrane protein mitofilin controls cristae morphology. *Mol. Biol. Cell* **16,** 1543–1554.
Johnson, R. P. C. (1969). Crystalline fibrils and complexes of membranes in the parietal layer in sieve elements. *Planta* **84,** 68–80.
Johnson, J. E., Mehler, W. R., and Miquel, J. (1975). A fine structure study of degenerative changes in the dorsal column nuclei of aging mice. Lack of protection by vitamin E. *J. Gerontol.* **30,** 395–411.
Jung, B., Moritz, M. E., and Berchtold, J. P. (1981). Fine structure and function of interrenal (adrenocortical) cells of dexamethasone-treated trout (Salmo fario L.). *Cell Tissue Res.* **214,** 641-649.
Kalt, M. R. (1974). Mitochondrial pleomorphism in sustentacular cell of *Xenopus laevis*. *Anat. Rec.* **182,** 53–60.

Karasaki, S. (1970). An electron microscope study of intranuclear canaliculi in Novikoff hepatoma cells. *Cancer Res.* **30,** 1736–1742.

Kartenbeck, J., Stukenbrok, H., and Helenius, A. (1989). Endocytosis of simian virus 40 into the endoplasmic reticulum. *J Cell Biol.* **109,** 2721–2729.

Kaup, F. J., Bruno, S. F., Mätz-Rensing, K., and Schneider, T. (2005). Tubuloreticular structures in rectal biopsies of SIV-infected rhesus monkeys (*Macaca mulatta*). *Ultrastruct Pathol.* **29,** 357–366.

Kessel, R. G. (1983). The structure and function of annulate lamellae: Porous cytoplasmic and intranuclear membranes. *Int. Rev. Cytol.* **82,** 181–303.

Kessel, R. G. (1990). A novel and transient structure associated with annulate lamellae morphogenesis: The Necturus oocyte revisited. *J. Submicrosc. Cytol. Pathol.* **22,** 551–564.

Kessel, R. G. (1992). Annulate lamellae: A last frontier in cellular organelles. *Int. Rev. Cytol.* **133,** 43–120.

Kessel, R. G., and Beams, H. W. (1965). An unusual configuration of the Golgi complex in pigment-producing "test" cells of the ovary of the tunicate, Styela. *J. Cell Biol.* **25,** 55–67.

Kessel, R. G., and Beams, H. W. (1968). Intranuclear membranes and nuclear-cytoplasmic exchange in young crayfish oocytes. *J. Cell Biol.* **39,** 735–741.

Kim, K. S. W., and Boatman, E. S. (1967). Electron microscopy of monkey kidney cell cultures infected with rubella virus. *J. Virol.* **1,** 205–214.

Knabe, W., and Kuhn, H.-J. (1996). Morphogenesis of megamitochondria in the retinal cone inner segments of *Tupaia belangeri* (Scandentia). *Cell Tissue Res.* **285,** 1–9.

Knabe, W., Skatchkov, S., and Kuhn, H.-J. (1997). "Lens mitochondria" in the retinal cones of the tree shrew *Tupaia belangeri*. *Vision Res.* **37,** 267–271.

Kochevar, D. T., and Anderson, R. G. (1987). Purified crystalloid endoplasmic reticulum from UT-1 cells contains multiple proteins in addition to 3-hydroxy-3-methylglutaryl coenzyme A reductase. *J. Biol. Chem.* **262,** 10321–10326.

Koestner, A., Kasza, L., and Holman, J. E. (1966). Electron microscopic evaluation of the pathogenesis of porcine polioencephalomyelitis. *Am. J. Pathol.* **49,** 325–337.

Kohorn, E. I., Rice, S. I., Hemperly, S., and Gordon, M. (1972). The relation of the structure of progestational steroids to nucleolar differentiation in human endometrium. *J. Clin. Endocrinol.* **34,** 257–264.

Kostianovsky, M., Orenstein, J. M., Schaff, Z., and Grimley, P. M. (1987). Cytomembranous inclusions observed in acquired immuno-deficiency syndrome. *Arch. Pathol. Lab. Med.* **111,** 218–223.

Kuwabara, T. (1979). Photic and photo-thermal effects on the retinal pigment epithelium. *In* : "The Retinal Pigment Epithelium" (K. M. Zinn and M. F. Marmor, Eds.), pp. 293–313. Harvard University Press, Cambridge.

Landh, T. (1994). Phase Behavior in the System Pine Needle Oil Monoglycerides-Poloxamer 407- Water at 20°. *J. Phys. Chem.* **98,** 8453–8467.

Landh, T. (1995). From entangled membranes to eclectic morphologies: Cubic membranes as subcellular space organizers. *FEBS Lett.* **369,** 13–17.

Landh, T. (1996). Cubic cell membrane architectures. Taking another look at membrane bound cell spaces. PhD thesis, p. 188. Lund University, Sweden.

Lang, N. J. (1965). Electron microscopy study of heterocyst development in *Anaebaena azollae* Strasburger. *J. Phycol.* **1,** 127–134.

Lang, N. J., and Rae, P. M. M. (1967). Structures in a blue-green alga resembling pro-lamellar bodies. *Protoplasma* **64,** 67–74.

Langenberg, W. G., and Schroeder, H. F. (1973). Endoplasmic reticulum-derived pinwheels in wheat infected with wheat spindle streak mosaic virus. *Virology* **55,** 218–223.

Larsson, K. (1989). Cubic lipid-water phases: Structures and biomembrane aspects. *J. Phys. Chem.* **93,** 7304–7314.

Larsson, K., Fontell, K., and Krog, N. (1980). Structural relationships between lamellar, cubic and hexagonal phases in monoglyceride-water systems. Possibility of cubic structures in biological systems. *Chem. Phys. Lipids* **27,** 321–328.

Leeson, C. R., and Leeson, T. S. (1969). Mitochondrial organization in skeletal muscle of the rat soft palate. *J. Anat.* **105,** 363–370.

Leonard, J. B., and Summers, R. G. (1976). The ultrastructure of the integument of the American eel, *Anguilla rostrata*. *Cell Tissue Res.* **171,** 1-30.

Li, S. J., Yamashita, Y., and Yamazaki, M. (2001). Effect of electrostatic interactions on phase stability of cubic phases of membranes of monoolein/dioleoylphosphatidic acid mixtures. *Biophys. J.* **81,** 983–993.

Linder, J. C., and Staehelin, L. A. (1980). The membrane lattice: A novel organelle f the trypanosomatid flagellate Leptomonas collosoma. *J. Ultrastruct. Res.* **72,** 200–205.

Locket, N. A. (1973). Retinal structure in *Latimeria chalumnae*. *Phil. Trans. R. Soc. Lond. B* **266,** 493–518.

Lohner, K. (1996). Is the high propensity of ethanolamine plasmalogens to form non-lamellar lipid structures manifested in the properties of biomembranes? *Chem. Phys. Lipids* **81,** 167–184.

Lucas, W. J., and Franceshi, V. R. (1981). Characean charasome-complex and plasmalemma vesicle development. *Protoplasma* **107,** 255–267.

Lucic, V., Forster, F., and Baumeister, W. (2005). Structural studies by electron tomography: From cells to molecules. *Annu. Rev. Biochem.* **74,** 833–865.

Luzzati, V. (1997). Biological significance of lipid polymorpholism: The cubic phase commentary. *Curr. Opin. Struct. Biol.* **7,** 661–668.

Lüllmann-Rauch, R., and Reil, G. H. (1973). Chlorphentermine-induced ultrastructural changes in liver tissues of four animal species. *Virchows Arch. B Zellpathol.* **13,** 307–320.

Macdonald, R. D., and Engel, A. G. (1970). Experimental chloroquine myopathy. *J. Neuropathol. Exp. Neurol.* **29,** 479–499.

Mackenzie, J. M., Khromykh, A. A., and Parton, R. G. (2007). Cholesterol manipulation by West Nile virus perturbs the cellular immune response. *Cell Host Microbe* **2,** 229–239.

Madarame, H., Fujimoto, Y., and Moriguchi, R. (1986). Ultrastructural studies on muscular atrophy in Marek's disease. I. Denervation atrophy in chicken skeletal muscle. A light and electron microscopic study. *Jpn. J. Vet. Res.* **34,** 25–49.

Maldovan, M., Urbas, A. M., Yufa, N., Carter, W. C., and Thomas, E. L. (2002). Photonic properties of bicontinuous cubic microphases. *Phys. Rev. B* **65,** 165123.49.

Mannella, C. A. (2006). Structure and dynamics of the mitochondrial inner membrane cristae. *Biochim. Biophys. Acta* **17,** 542–548.

Mantovani, G., Santa Cruz, G., Piso, A., Arangino, V., Balestrieri, A., and Del Giacco, G. S. (1986). Hairy cell leukemia with ultrastructural finding of 'tubuloreticular inclusions' in hairy cells: A possible marker of a virus-induced disease? *J. Submicrosc. Cytol.* **18,** 617–624.

Marchal, T., Dezutter-Dambuyant, C., Fournel, C., Magnol, J. P., and Scmitt, D. (1995). Immunophenotypic and ultrastructural evidence of the langerhans cell origin of the canine cutanous histiocytoma. *Acta Anat.* **153,** 189–202.

Marquart, K. H. (2005). Occurrence of tubuloreticular structures and intracisternal paracrystalline inclusions in endothelial cells of tissue from different epidemiological types of Kaposi's sarcoma. *Ultrastruct. Pathol.* **29,** 85–93.

de Martino, C., Accini, L., and Andres, G. A. (1969). Tubular structures associated with the endothelial endoplasmic reticulum in glomerular capillaries of rhesus monkey and nephritic man. *Z. Zellforsch.* **97,** 502–511.

Mastaglia, F. L., and Walton, J. N. (1992). Inflammatory myopathies. *In*: "Skeletal Muscle Pathology" (F. L. Mastaglia and J. N. Walton, Eds.), pp. 453–491, Churchill Livingstone, Edinburgh.

Masum, S. M., Li, S. J., Awad, T. S., and Yamazaki, M. (2005). Effect of positively charged short peptides on stability of cubic phases of monoolein/dioleoylphosphatidic acid mixtures. *Langmuir* **21,** 5290–5297.

Mays, U. (1967). Paracrystalline endoplasmic reticulum in ovaries of the Pyrrhocoris apterus (*Heteroptera*). *Z. Naturforschg. B* **22,** 459.

Mckanna, J. A. (1976). Fine structure of fluid segregation organelles of *Paramecium* contractile vacuoles. *J. Ultrastruct. Res.* **54,** 1–10.

McLean, R. J., and Pessoney, G. F. J. (1970). A large scale quasi-crystalline lamellar lattice in chloroplasts of the green alga *Zygnema. J. Cell Biol.* **45,** 522–531.

McNutt, N. S., and Jones, A. L. (1970). Observations on the ultrastructure of cytodifferentiation in the human fetal adrenal cortex. *Lab. Invest.* **22,** 513–527.

Mendoza, A. S., and Kühnel, W. (1989). Light- and electron microscopical studies on the vomeronasal organ (VNO) of the newborn guinea pig. *Z. Mikroskop. Anat. Forsch.* **103,** 801–806.

Menke, W. (1962). Über die Struktur der Heitz-Leyonschen Kristalle. *Z. Naturforschg.* **17b,** 188–190.

Menke, W. (1963). Zur Stereometrie der Heitz-Leyonschen Kristalle von Chlorophytum comosum. *Z. Naturforschg.* **18b,** 821–826.

Miike, T., Ohtani, Y., Tamari, H., Ishitsu, T., and Nonaka, I. (1984). An electron microscopical study of the T-system in biopsied muscles from Fukuyama type congenital muscular dystrophy. *Muscle Nerve* **7,** 629–635.

Miledi, R., and Slater, C. (1969). Electron-microscopic structure of denervated skeletal muscle. *R. Proc. Roy. Soc. Lond. B.* **174,** 253–269.

Miller, O. L. (1966). Structure and composition of peripheral nucleoli of salamander oocytes. *Natl. Cancer Inst. Monogr.* **23,** 53–66.

Moore, G. E., and Chandra, S. (1968). Is degos' disease of viral origin? *Lancet* **2,** 406.

Moxey, P. C., and Trier, J. S. (1979). Development of villus absorptive cells in the human fetal small intestine: A morphological and morphometric study. *Anat. Rec.* **195,** 463–482.

Munroe, J. S., Shipkey, F., Erlandson, R. A., and Windle, W. F. (1964). Tumors induced in juvenile and adult primates by chicken sarcoma virus. *Natl. Cancer Monogr.* **17,** 365–390.

Murakami, S., Yamada, N., Nagano, M., and Osumi, M. (1985). Three-dimensional structure of the prolamellar body in squash etioplasts. *Protoplasma.* **128,**147-156.

Murmains, L., and Evert, R. F. (1966). Some aspects of sieve cell ultrastructure in *Pinus strobus. Am. J. Bot.* **53,** 1065–1078.

Murphy, F. A., Harrison, A. K., Gary, G. W., Whitfiled, S. G., and Forrester, F. T. (1968). St. Louis encephalitis virus infection of mice. *Lab. Invest.* **19,** 652–662.

Murray, A. B., Büscher, H., Erfle, V., Biehl, T., and Gössner, W. (1983). Intranuclear undulating membranous structures in cells of a human parosteal osteosarcoma. *Ultrastruct. Pathol.* **5,** 163–170.

Nagan, N., and Zoeller, R. A. (2001). Plasmalogens: Biosynthesis and functions. *Prog. Lipid Res.* **40,** 199–229.

Nagan, N., Hajra, A. K., Larkins, L. K., Lazarow, P., Purdue, P. E., Rizzo, W. B., and Zoeller, R. A. (1998). Isolation of a Chinese hamster fibroblast variant defective in dihydroxyacetonephosphate acyltransferase activity and plasmalogen biosynthesis: Use of a novel two-step selection protocol. *Biochem. J.* **332,** 273–279.

Nakamura, R. M. (1974). Immunopathology: Clinical Laboratory Concepts and Methods Little, Brown and Co, Boston.

Neuwirth, M., Daly, J. W., Myers, C. W., and Tice, L. W. (1979). Morphology of the granular secretory glands in skin of poison-dart frogs *(Dendrobatidae). Tissue Cell* **11,** 755–771.

Newcomb, E. H. J. (1967). Fine structure of protein-storing plastids in bean root tips. *J. Cell Biol.* **33,** 143–163.

Nicolas, G. (1991). Advantages of fast-freeze fixation followed by freeze-substitution for the preservation of cell integrity. *J. Electron. Microsc. Tech.* **18,** 395–405.
Nicolas, M.-T. (1979). Prcsénce de photosomes dans les fractions lumineuses du système élytral des Polynoïnae. *C. R. Acad. Sci. Paris D* **289,** 177–180.
Nilsson, J. (1969). The fine structure of *Neobursaridium gigas* (Balech). *Compt. Rend. Trav. Lab. Carlsberg.* **37,** 49–76.
Norback, D. H., and Allen, J. R. (1969). Morphogenesis of toxic fat-induced concentric membrane arrays in rat hepatocytes. *Lab. Invest.* **20,** 338–346.
Northcote, D. H., and Wooding, F. B. P. (1966). Development of sieve tubes in *Acer pseudoplatanus*. *Proc. Roy. Soc. B* **163,** 524–537.
Nunez, E. A., and Gershon, M. D. (1981). Specific paracrystalline structures of rough endoplasmic reticulum in the follicular (stellate) cells of the dog adenohypophysis. *Cell Tissue Res.* **215,** 215–221.
Öhman, P. (1974). Fine structure of the retinal pigment epithelium of the river lamprey (*Lampetra fluviatilis*). *Acta Zool.* **55,** 245–253.
Okamoto, Y., Masum, S. M., Miyazawa, H., and Yamazaki, M. (2008). Low-pH-induced transformation of bilayer membrane into bicontinuous cubic phase in dioleoylphosphatidylserine/monoolein membranes. *Langmuir* **24,** 3400–3406.
Oparka, K. J., and Johnson, P. C. (1978). Endoplasmic reticulum and crystalline fibrils in the root protophloem of Nymphoides peltata. *Planta* **143,** 21–27.
Orci, L., Brown, M. S., Goldstein, J. L., Garcia-Segura, L. M., and Anderson, R. G. (1984). Increase in membrane cholesterol: A possible trigger for degradation of HMG CoA reductase and crystalloid endoplasmic reticulum in UT-1 cells. *Cell* **36,** 835–845.
Osumi, M., Yamada, N., Nagano, M., Murakami, S., Baba, N., Oho, E., and Kanaya, K. (1984). Three-dimensional observation of the prolamellar bodies in etioplasts of squash Cucurbita moschata. *Scan. Electron Microsc.* **1,** 111–119.
Pappas, G. D., and Brandt, P. W. (1959). Mitochondria. I. Fine structure of the complex patterns in the mitochondria of Pelomyxa carolinensis Wilson (*Chaos chaos L.*). *J. Biophys. Biochem. Cytol.* **6,** 85–90.
Pappas, G. D., Peterson, E. R., Masurovsky, E. B., and Crain, S. M. (1971). Electron microscopy of the in vitro development of mammalian motor end plates. *Ann. N.Y. Acad. Sci.* **83,** 33–45.
Parthasarathy, M. V. (1974a). Ultrastructure of phloem in palms II. Structural changes, and fate of the organelles in differentiating sieve elements. *Protoplasma* **79,** 93–125.
Parthasarathy, M. V. (1974b). Ultrastructure of phloem in palms III. Mature phloem. *Protoplasma* **79,** 265–315.
Parton, R. G., Way, M., Zorzi, N., and Stang, E. (1997). Caveolin-3 associates with developing T-tubules during muscle differentiation. *J. Cell Biol.* **136,** 137–154.
Pathak, R. K., Luskey, K. L., and Anderson, G. W. (1986). Biogenesis of the crystalloid endoplasmic reticulum in UT-1 cells: Evidence that newly formed endoplasmic reticulum emerges from the nuclear envelope. *J. Cell Biol.* **102,** 2158–2168.
Patterson, D. J. (1980). Contractile vacuoles and associated structures: Their organization and function. *Biol. Rev.* **55,** 1–46.
Pellegrino, C., and Franzini, C. (1963). An electron microscope study of denervation atrophy in red and white skeletal muscle fibers. *J. Cell Biol.* **17,** 327–349.
Pfeifer, U., Thomssen, R., Legler, K., Böttcher, U., Gerlich, W., Weinmann, E., and Klinge, O. (1980). Experimental non-A, non-B hepatitis: Four types of cytoplasmic alteration in hepatocytes ot infected chimpanzees. *Virchows Arch. B. Cell Pathol.* **33,** 233–243.
Pisam, M., Boeuf, G., Prunet, P., and Rambourg, P. (1990). Ultrastructural features of mitochondria-rich cells in stenohaline freshwater and seawater fishes. *Am. J. Anat.* **187,** 21–31.

Pisam, M., Le Moal, C., Auperin, B., Prunet, P., and Rambourg, A. (1995). Apical structures of "mitochondria-rich" α and ß cell in euryhalinc fish gill: Their behavior in various living conditions. *Anat. Rec.* **241,** 13–24.

Ponzi, R., Pizzolongo, P., and Caputo, G. (1978). Ultrastructure particularities in ovular tissues of some rhoedales taxa ad their probable taxonomic value. *J. Submicrosc. Cytol.* **10,** 81–88.

Pospischil, A., and Bachmann, P. A. (1980). Nuclear changes in cells infected with parapoxviruses stomatitis papulosa and orf: An *in vivo* and *in vitro* ultrastructural study. *J. Gen. Virol.* **47,** 113–121.

Profant, D. A., Roberts, C. J., and Wright, R. L. (2000). Mutational analysis of the karmellae-inducing signal in Hmg1p, a yeast HMG-CoA reductase isozyme. *Yeast* **16,** 811–827.

Quan, C. M., and Doane, F. W. (1983). Ultrastructural evidence for the cellular uptake of rotavirus by endocytosis. *Intervirology* **20,** 223–231.

Reichle, R. E. (1972). Fine structure of Oedogoniomyces zoospores, with comparative observations of *Monoblepharella zoospores*. *Can. J. Bot.* **50,** 819–824.

Reynolds, E. S., and Ree, H. J. (1971). Liver parenchymal cell injury. VII. Membrane denaturation following carbon tetrachloride. *Lab. Invest.* **25,** 269–278.

Robert, D. (1969a). Evolution de quelques organites cytoplasmiques au cours de la maturation de l'oosphére de *Selaginella Kraussiana* A. Br. *C. R. Acad. Sci. (Paris) Serie D* **268,** 2775–2778.

Robert, D. (1969b). Organisation du réticulum endoplasmique dans le cytoplasme basal de l'oosphére de *Selaginella Kraussiana* A. Br. *C. R. Acad. Sci. (Paris) Serie D* **269,** 2341–2344.

Robinson, D. G. (1985). Plant Membranes. Endo and Plasma Membranes of Plant Cells Wiley, New York.

Rohlich, P., and Torok, L. J. (1963). The fine structure of the eye of the Weinberg snail (*Helix pomatia* L.). *Z. Zellforsch. Mikrosk. Anat.* **60,** 348–368.

Roitelman, J., Olender, E. H., Bar-Nun, S., Dunn, W. A. Jr., and Simoni, R. D. (1992). Immunological evidence for eight spans in the membrane domain of 3-hydroxy-3-methylglutaryl coenzyme A reductase: Implications for enzyme degradation in the endoplasmic reticulum. *J. Cell Biol.* **117,** 959–973.

Rowden, G. (1968). Aryl sulfatase in the sebaceous glands of mouse skin. *J. Invest. Dermatol.* **51,** 41–50.

Ruebner, B. H., Hirano, T., and Slusser, R. J. (1967). Electron microscopy of the hepatocellular and Kupffer-cell lesions of mouse hepatitis, with particular reference to the effect of cortisone. *Am. J. Pathol.* **51,** 163–189.

Ruebner, B. H., Moore, J., Rutherford, R. B., Seligman, A. M., and Zuidema, G. D. (1969). Nutritional cirrhosis in rhesus monkeys: Electron microscopy and histochemistry. *Exp. Mol. Pathol.* **11,** 53–70.

Russel, L., and Burguet, B. (1977). Ultrastructural of Leydig cells as revealed by secondary tissue treatment with ferrocyanide-osmium mixture. *Tissue Cell* **9,** 751–766.

Ryberg, M., Sandelius, A. S., and Selstam, E. (1983). Lipid composition of prolamellar bodies and prothylakoids of wheat etioplasts. *Physiol. Plant.* **57,** 555–560.

Sandig, G., Eärgel, E., Menzel, F., Vogel, F., Zimmer, T., and Schunck, W.-H. (1999). Regulation of endoplasmic reticulum biogenesis in response to cytochrome P450 overproduction. *Drug Metab. Rev.* **31,** 393–410.

Sasaki, F., Horiguchi, T., Takahama, H., and Watanabe, K. (1985). Network and lamellar structures in the tail muscle fibers of the metamorphosing anuran tadpole. *Anat. Rec.* **211,** 369–375.

Samorajski, T., Ordy, J. M., and Keefe, J. R. (1966). Structural organization of the retina in the tree shrew (*Tupaia glis*). *J. Cell Biol.* **28,** 489–504.

Schaff, Z., Lapis, K., and Grimley, P. M. (1976). Undulating membranous structures associated with the endoplasmic reticulum in tumour cells. *Int. J. Cancer* **18,** 697–702.
Schaff, Z., Eder, G., Eder, C., and Lapis, K. (1992). Ultrastructure of normal and hepatitis virus infected human and chimpanzee liver: Similarities and differences. *Acta Morphol. Hung.* **40,** 203–214.
Schuster, F. L. (1965). A deoxyribose nucleic acid component in mitochondria of *Didymium nigripes*, a slime mold. *Exp. Cell Res.* **39,** 329–345.
Sedar, A. W., and Rudzinska, M. A. (1956). Mitochondria of protozoa. *J. Biophys. Biochem. Cytol.* **2,** 331–334.
Seddon, A. M., Curnow, P., and Booth, P. J. (2004). Membrane proteins, lipids and detergents: Not just a soap opera. *Biochim. Biophys. Acta* **1666,** 105–117.
Seifert, K. (1971). Light and electron microscopic studies on the organ of Jacobson (vomero-nasal organ) of cats. *Arch Klin Exp Ohren Nasen Kehlkopfheilkd.* **200,** 223–251.
Seifert, K. (1972). New results of light- and electron-microscopic studies of the peripheral olfactory organ including the Bowman glands and vomero-nasal organ. *Acta Otorhinolaryngol Belg.* **26,** 463–492.
Seifert, K. (1973). An unknown differentiation of membranes in cells of Jacobson's organ of the cat. *Z. Zellforsch.* **140,** 583–586.
Seman, G., Gallager, H. S., Lukeman, J. M., and Dmochowski, L. (1971). Studies on the presence of particles resembling RNA virus particles in human breast tumors, pleural effusions, their tissue cultures, and milk. *Cancer* **28,** 1431–1442.
Senisterra, G., and Epand, R. M. (1993). Role of membrane defects in the regulation of the activity of protein kinase C. *Arch. Biochem. Biophys.* **300,** 378–383.
Singla, C. L. (1975). Ultrastructure of the eyes of *Arctonoë vittata* Grube (*Polychaeta, Polynoidae*). *J. Ultrastruct. Res.* **52,** 333–339.
Sisson, J. K., and Fahrenbach, W. H. (1967). Fine structure of steroidogenic cells of a primate cutaneous organ. *Am. J. Anat.* **121,** 337–368.
Smith, D. S. (1963). The structure of flight muscle sarcosomes in the blowfly *Calliphora erythrocephala* (Diptera). *J. Cell Biol.* **19,** 115–138.
Smith, R. D., and Deinhardt, F. (1968). Unique cytoplasmic membranes in rous sarcoma virus-induced tumors of a subhuman primate. *J. Cell. Biol.* **37,** 819–823.
Snapp, E. L., Hegde, R. S., Francolini, M., Lombardo, F., Colombo, S., Pedrazzini, E., Borgese, N., and Lippincott-Schwartz, J. (2003). Formation of stacked ER cisternae by low affinity protein interactions. *J. Cell Biol.* **163,** 257–269.
Somogyi, E., Varga, T., and Sótonyi, P. (1971). Mononuclear-cell inclusion bodies in dogs treated with A.L.S. *Lancet* **2,** 605–606.
Spicer, S. S., Parmely, R. T., Boyd, L., and Schulte, B. A. (1990). Giant mitochondria distinct from enlarged mitochondria in secretory and ciliated cells of gerbil trachea and bronchioles. *Am. J. Anat.* **188,** 269–281.
Stang-Voss, C. (1972). Ultrastructural equivalents of cellular autophagy. Electron microscopical observations on spermatids of *Eisenia foetida* during the cytoplasmic reduction. *Z. Zellforsch.* **127,** 580–590.
Starke, F.-J., and Nolte, A. (1970). Tubular bodies in the cytoplasm of spermatids of *Planorbarius corneus* L. (Basommatophora). *Z. Zellforsch.* **105,** 210–221.
Stoebner, P., Sengel, A., and Badina, J. J. (1972). Tubular inclusions. Discovery in endothelial cells of a subcutaneous myxoma. *Nouv Presse Med.* **1,** 1149–1150.
Strauss, M., Hofhaus, G., Schröder, R. R., and Kühlbrandt, W. (2008). Dimer ribbons of ATP synthase shape the inner mitochondrial membrane. *EMBO J.* **27,** 1154–1160.
Szakacs, J. E., Kasnic, G., and Walling, A. K. (1991). Soft tissue sarcoma with complex membranous and microtubular inclusions. *Ann. Clin. Lab. Sci.* **21,** 430–440.

Tahmisian, T. N., Powers, E. L., and Devine, R. L. (1956). Light and electron microscope studies of morphological changes of mitochondria during spermatogenesis in the grasshopper. *J. Biophys. Biochem. Cytol.* **2,** 325–329.

Tahmisian, T. N., and Devine, R. L. (1961). The influence of X-rays on organelle induction and differentiation in grasshopper spermatogenesis. *J. Biophys. Biochem. Cytol.* **9,** 29–45.

Takei, K., Mignery, G. A., Mugnaini, E., Südhof, T. C., and de Camilli, P. (1994). Inositol 1,4,5-trisphosphate receptor causes formation of ER cisternal stacks in transfected fibroblasts and in cerebellar Purkinje cells. *Neuron* **12,** 327–342.

Tandler, B., and Erlandson, R. A. (1983). Giant mitochondria in a pleomorphic adenoma of the submandibular gland. *Ultrastruct. Pathol.* **4,** 85–96.

Tandler, B., and Moribier, L. G. (1974). Ultrastructure of pseudochromes and calottes in spermatogenic cells of the backswimmer, *Notonecta undulata* (Say). *Tissue Cell* **6,** 557–572.

Tandler, B., Erlandson, R. A., and Southam, C. M. (1973). Unusual membrane formations in HEp-2 cells infected with Ilheus virus. *Lab. Invest.* **28,** 217–223.

Tanuma, Y. (1983). Occurrence of crystalloids in the sinusoidal endothelial cell of a crab-eating monkey liver. *Arch. Histol. Jpn.* **46,** 523–531.

Thorsch, J., and Esau, K. (1981). Changes in the endoplasmic reticulum during differentiation of a sieve element in *Gossypium hirsutum*. *J. Ultrastruct. Res.* **74,** 183–194.

Tinari, A., Ammendolia, M. G., Superti, F., and Donelli, G. (1996). Tubuloreticular structures induced by rotavirus infection in HT-29 cells. *Ultrastruct. Pathol.* **20,** 571–576.

Toyoshima, K., and Tandler, B. (1987). Modified smooth endoplasmic reticulum in type II cells of rabbit taste buds. *J. Submicrosc. Cytol.* **19,** 85–92.

Tripodi, G., and de Masi, F. (1977). The post-fertilization stages of red-algae: The fine structure of the fusion cell of *Erythrocystis*. *J. Submicrosc. Cytol.* **9,** 389–401.

Urbas, A. M., Maldovan, M., DeRege, P. P., and Thomas, E. L. (2002). Bioconcinuous cubic block copolymer photonic crystals. *Adv. Mater.* **14,** 1850–1853.

Uzman, B. G., Saito, H., and Kasac, M. (1971). Tubular arrays in the endoplasmic reticulum in human tumor cells. *Lab. Invest.* **24,** 492–498.

van Lennep, E. W., and Lanzing, W. J. (1967). The ultrastructure of glandular cells in the external dendritic organ of some marine catfish. *J. Ultrastruct. Res.* **18,** 333-344.

Vergères, G., Yen, T. S., Aggeler, J., Lausier, J., and Waskell, L. (1993). A model system for studying membrane biogenesis. Overexpression of cytochrome b5 in yeast results in marked proliferation of the intracellular membrane. *J. Cell Sci.* **106,** 249–259.

Voeltz, G. K., Prinz, W. A., Shibata, Y., Rist, J. M., and Rapoport, T. A. (2006). A class of membrane proteins shaping the tubular endoplasmic reticulum. *Cell* **124,** 573–586.

Voeltz, G. K., and Prinz, W. A. (2007). Sheets, ribbons and tubules—How organelles get their shape. *Nat. Rev. Mol. Cell Biol.* **8,** 258–264.

Walz, B. (1982). Ca^{2+}-sequestering smooth endoplasmic reticulum in an invertebrate photoreceptor. I. Intracellular topography as revealed by OsFeCN staining and in situ Ca accumulation. *J. Cell. Biol.* **93,** 839–848.

Wehrmeyer, W. (1965a). On the crystal structure of the so called prolamellar body in proplastids of etiolated beans. I. Pentagondodecaeder as center of concentric prolamellar body. *Z. Naturforsch.* **20b,** 1270–1278.

Wehrmeyer, W. (1965b). On the crystal structure of the so called prolamellar body in proplastids of etiolated beans. II. Wurtzit lattice as a tubular model of the prolamellar body. *Z. Naturforsch.* **20b,** 1288–1296.

Wehrmeyer, W. (1965c). On the crystal structure of the so called prolamellar body in proplastids of etiolated beans. II. Zincblende as a tubular model of the prolamellar body. *Z. Naturforsch.* **20b,** 1278–1288.

Weier, T. E., and Brown, D. L. (1970). Formation of the prolamellar body in 18-day, dark-grown seedlings. *Am. J. Bot.* **57,** 267–275.

Weiner, J. H., Lemire, B. D., Elmes, M. L., Bradley, R. D., and Scraba, D. G. (1984). Overproduction of fumarate reductase in *Escherichia coli* induces a novel intracellular lipid-protein organelle. *J. Bacteriol.* **158,** 590–596.

Wells, K. (1972). Light and electron microscopic studies of *Ascobolus stercorarius*. II. Ascus and ascospore ontogeny. *Univ. Calif. Publ. Bot.* **62,** 1–93.

Welsch, U. (1968). The fine structure of Joseph cells in the brain of Amphioxus. *Z. Zellforsch.* **86,** 252–261.

Wolf, K. W., and Motzko, D. (1995). Paracrystalline endoplasmic reticulum is typical of gametogenesis in Hemiptera species. *J. Struct. Biol.* **114,** 105–114.

Wooding, F. B. P. (1966). The development of the sieve elements of Pinus pinea. *Planta* **69,** 230–243.

Wooding, F. B. P. (1967). Endoplasmic reticulum aggregates of ordered structure. *Planta* **76,** 205–208.

Wright, R., Basson, M., D'Ari, L., and Rine, J. (1988). Increased amounts of HMG-CoA reductase induce "karmellae": A proliferation of stacked membrane pairs surrounding the yeast nucleus. *J. Cell Biol.* **107,** 101–114.

Yamamoto, A., Masaki, R., and Tashiro, Y. (1996). Formation of crystalloid endoplasmic reticulum in COS cells upon overexpression of microsomal aldehyde dehydrogenase by cDNA transfection. *J. Cell Sci.* **109,** 1727–1738.

Yorke, M. A., and Dickson, D. H. (1985). Lamellar to tubular conformational changes in the endoplasmic reticulum of the retinal pigment epithelium of the newt, Notophtalmus viridescens. *Cell Tissue Res.* **241,** 629–637.

Youssef, N. N., and Hammond, D. M. (1971). The fine structure of the developmental stages of the microsporidian Nosema apis Zander. *Tissue Cell* **3,** 283–294.

Zachariah, K. (1970). Lattice bodies and filament bundles in apothecial cells of the fungus *Ascobolus*. *Can. J. Bot.* **48,** 1115–1118.

Zachariah, K., and Anderson, R. H. (1973). On the distribution and development of lattice bodies in apothecial cells of the fungus Ascobolus. *J. Ultrastruct. Res.* **44,** 405–420.